Heliyon 9 (2023) e21935

Contents lists available at ScienceDirect

Heliyon

journal homepage: www.cell.com/heliyon

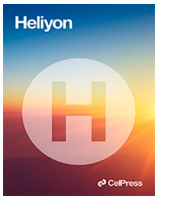

HuangQi ChiFeng decoction maintains gut microbiota and bile acid homeostasis through FXR signaling to improve atherosclerosis

Jiaqi Fu, Yuqin Liang, Yunhe Shi, Donghua Yu, Yu Wang, Pingping Chen, Shumin Liu, Fang Lu *

Institute of Traditional Chinese Medicine, Heilongjiang University of Chinese Medicine, Harbin, Heilongjiang, China

ARTICLE INFO

Keywords:
Atherosclerosis
HQCFT
Bile acid
Gut microbiota
FXR
LXRα

ABSTRACT

Huangqi Chifeng Decoction (HQCFT), a traditional Chinese medicine preparation, has long been used to treat cardiovascular and cerebrovascular diseases. However, the mechanism of the beneficial effect of HQCFT on atherosclerosis remains to be explored. In this work, to investigate the effects of HQCFT on bile acid (BA) metabolism and the gut microbiome in atherosclerosis, ApoE$^{-/-}$ mice were fed a with high-fat diet for 16 weeks to establish the AS model. HQCFT(1.95 g kg^{-1} and 3.9 g kg^{-1} per day) was administered intragastrically for 8 weeks to investigate the regulatory effects of HQCFT on gut microbiota and bile acid metabolism and to inhibit the occurrence and development of AS induced by a high-fat diet. Histopathology, liver function and blood lipids were used to assess whether HQCFT can reduce plaque area, regulate lipid levels and alleviate liver steatosis in AS mice. In addition, 16S rDNA sequencing was used to screen the gut microbiota structure, and ultrahigh-performance liquid chromatography-tandem mass spectrometry (UPLC–MS/MS) was used to determine the bile acid profile. The mRNA and protein expression levels of bile acid metabolism were detected by RT–PCR and WB to find the potential correlation. Results: HQCFT can regulate gut microbiota disorders, which was achieved by increasing gut microbiota diversity and altering *Proteobacteria*, *Desulfobacterota*, *Deferribacteres*, *Rodentibacter*, *Parasutterella*, and *Mucispirillum* interference abundance to improve AS-induced gut microbiota. HQCFT can also adjust the content of bile acids (TCA, LCA, DCA, TDCA, TLCA, UDCA, etc.), regulate bile acid metabolism, relieve liver fat accumulation, and inhibit the process of AS. In addition, HQCFT can restore the abnormal metabolism of bile acid caused by AS by regulating the expression of farnesoid X receptor (FXR), liver X receptor α (LXRα), ABCA1, ABCG1 and CYP7A1. Conclusion: HQCFT may play a part in the prevention of atherosclerosis by inhibiting the FXR/LXRα axis, increasing the expression of CYP7A1 in the liver, and regulating the interaction between the gut microbiota and bile acid metabolism.

1. Introduction

Atherosclerosis (AS) is a major pathological process in most cardiovascular diseases, and one of its main pathogenic mechanisms is

* Corresponding author.
E-mail addresses: ShumLiu0321@163.com (S. Liu), lufang_1004@163.com (F. Lu).

https://doi.org/10.1016/j.heliyon.2023.e21935
Received 17 August 2023; Received in revised form 31 October 2023; Accepted 31 October 2023
Available online 8 November 2023

the deposition of oxidized LDL cholesterol in the lining of the arteries, which causes a continuous inflammatory response (increased secretion of inflammatory factors and inflammatory cells) and the progressive formation of atheromatous deposits in the lumen of the arteries [1,2]. Over time, the fibrosis of the atheromatous plaque in the arterial wall will gradually increase and accumulate calcium minerals, leading to narrowing of the lumen, loss of elasticity of the wall, and rupture of the plaque, causing thrombosis and blockage of the blood vessel, and eventually causing adverse cardiovascular events, such as myocardial infarction, stroke, and angina, etc., which seriously endanger human health [3]. Therefore, it is of great scientific value and practical importance to take effectual measures to prevent and treat the development of atherosclerosis.

HuangQi ChiFeng decoction is from the "Yilin Gaicuo." Huangqi Chifeng Decoction (HQCFT), a TCM prescription, is distinguished by its potential effect to regulate blood rheology, and blood lipids and promote blood circulation(Chinese Pharmacopoeia Commission, 2020). HQCFT is composed of Astragalus membranaceus (Fisch.) Bunge (syn. *Astragalus propinquus* Schischkin), Paeoniae Radix Rubra (Paeonia lactiflora Pall.) and Saposhnikovia divaricata (Turcz.) Schischk.(Radix Saposhnikoviae). The names of all plants have been checked(http://www.worldfloraonline.org). Pharmacological research has confirmed that HQCFT and its modified prescription attenuate blood stasis and effectively inhibit the inflammatory response of AS-related cerebral infarction [4,5]. The clinical trials proved that HQCFT and its modified prescriptions reduce serum inflammatory factor levels in stroke patients with blood stasis and accelerate blood velocity in patients with AS-induced vertigo [6]. Most of these prescriptions have great antioxidant, anti-myocardial ischemia and immunoregulatory effects. Our previous study found that Huangqi Chifeng decoction could significantly improve cerebral edema, reduce the cerebral infarction area, and reduce the expression levels of a hypoxy-inducing factor (HIF-1α), NLRP3 inflammatory and cysteine aspartic protease-1 (Caspase-1) in brain tissue and serum in rats [7]. HQCFT can also play a role in treating cerebral infarction by improving the pathological changes in brain tissue, reducing the inflammatory response, promoting angiogenesis and regulating blood–brain barrier (BBB) function [8].

The traditional route of administration of Chinese medicine is mainly oral tonics, which inevitably encounter the gut microbiota in the organism, producing a two-way regulatory effect. Some Chinese medicines achieve therapeutic effects by restoring the structure and diversity of the gut microbiota to maintain homeostasis. The gut microbiota regulates many metabolic processes, including lipid metabolism, glucose metabolism and energy homeostasis [9]. A high-fat diet (HFD) is known to alter the composition of the gut microbiota, leading to disorders of lipid metabolism in humans [10],and disorders of lipid metabolism can further cause changes in the intestinal environment, leading to dysbiosis of the gut microbiota [11]. The gut microbiota can influence the development of AS in several ways. Dysbiosis leads to an inflammatory response that can exacerbate the development of AS plaques or lead to plaque rupture. In contrast, the gut microbiota affects the development of AS plaques by regulating cholesterol and lipid metabolism in the host [6].

As a critical endogenous signaling factor produced by the gut microbiota and host metabolism, bile acids(BAs) are critical regulators of body metabolism, not only in lipid uptake but also as important signaling molecules that regulate host metabolism and influence glucolipid metabolism and energy homeostasis [12]. The composition of the bile acid pool plays a crucial role in cholesterol homeostasis, and the bile acid receptor signaling pathway plays an important role in treating AS. BAs can limit hepatic bile acid synthesis by activating FXR to downregulate CYP7A1 expression [13]. BAs have therefore been considered as potential targets for AS prevention and treatment. Increasing the excretion of BAs and accelerating the elimination of lipids such as cholesterol positively affects the development of AS [14]. The rich and diverse modification of BAs by gut microbiota and the presence of the enterohepatic cycle allow BAs to act as a bridge between gut microbiota and the host, mediating interactions with the host [15]. In-depth studies on the relationship between bile acid metabolism and AS and the mechanisms of AS occurrence from different perspectives are of great significance in actively exploring the process of AS and new methods of prevention and treatment.

Therefore, in our study we used high-fat diet feeding to replicate the ApoE$^{-/-}$ mouse atherosclerosis model and HQCFT as an intervention to observe changes in liver histopathology, serum liver function, blood lipids and bile acid-related factors. With gut microbiota as the core of the study and bile acid metabolism as the main line of research, we explored the association between HQCFT regulation of gut microbiota and bile acid metabolism. The mechanism of HQCFT in treating AS is explored from the perspective of targeting gut microbiota to reverse the disorder of bile acid metabolism. This study provides new ideas for the prevention and treatment of AS and as well as a scientific basis for the clinical application of anti-AS.

2. Material and methods

2.1. Drugs and reagents

The daily dose of HQCFT for adults is 15 g, which is equivalent to including the following herbs: Astragalus membranaceus (Fisch.) Bunge (syn. *Astragalus propinquus* Schischkin), Paeoniae Radix Rubra (Paeonia lactiflora Pall.) and Saposhnikovia divaricata (Turcz.) Schischk. (Radix Saposhnikoviae). Our previous research [16]showed that HQCFT consists of the following dried herbal components: 30 g Astragalus membranaceus (Fisch.) Bunge, 9 g Paeoniae Radix Rubra, 6 g Saposhnikovia divaricata (Turcz.) Schischk were soaked in 8 vol of water for 30 min, decocted 3 times for 1 h each time, and concentrated with filtrate 3 times. The concentrated liquid was put into the lyophilization machine, and lyophilized powder with a paste extraction rate of 30.38 % was obtained, which was stored in drying dishes for later use. Furthermore, the HPLC of HQCFT extracts was established (Fig. S1).

The serum concentrations of alanine aminotransferase (ALT), aspartate aminotransferase (AST), alkaline phosphatase (ALP), total cholesterol (TC), triglycerides (TG), low-density lipoprotein cholesterol (LDL-C), and high-density lipoprotein cholesterol (HDL-C) were determined using a biochemical analyzer (Reddo Life Sciences Co., LTD, China). PrimeScript™ RT Reagent Kit with gDNA Eraser (Perfect Real Time) (TAKARA, Japan) and TB Green® Premix Ex Taq™ II (TAKARA, Japan) were used. GAPDH (#10494-1-AP), FXR

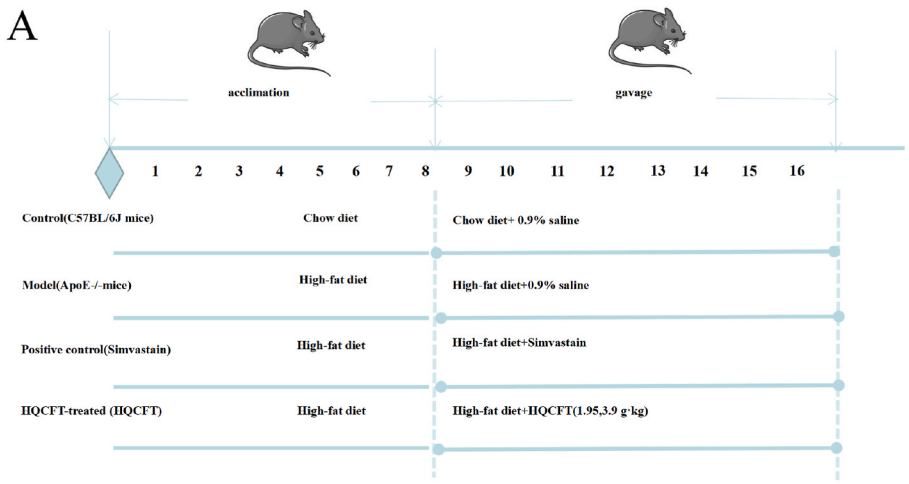

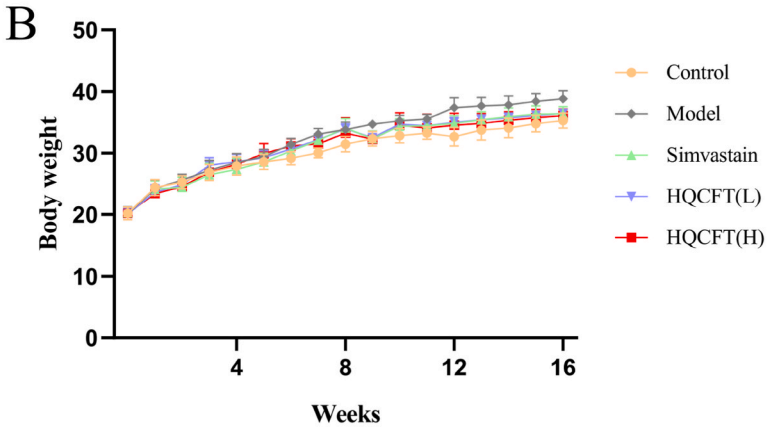

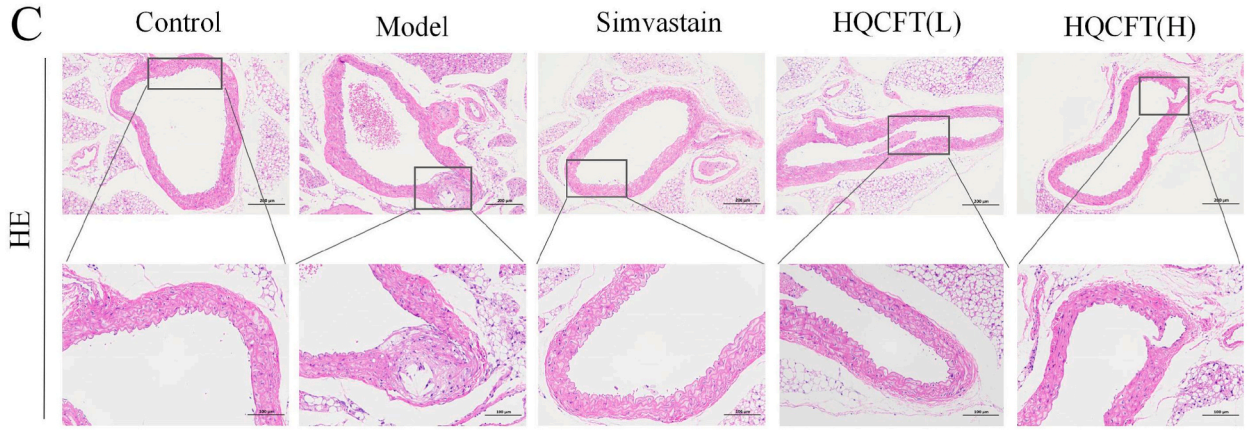

Fig. 1. Effects of HQCFT on HFD-induced ApoE$^{-/-}$ mice(n = 6). (A)The flow diagram of the experimental design.(B)Average body weight per group (n = 6 per group). (C)Representative images of H&E in aortic sections. (D–J) TC,TG,LDL-C,HDL-C,AST,ALT and ALP levels in the serum. (K) Representative images of liver histopathology(H&E and Oil red O). Data were expressed as mean ± SEM,and the statistically significant difference was analyzed by one-way ANOVA followed by Dunnett's multiple comparison tests. #$p < 0.05$, ##$p < 0.01$ via the control group; *$p < 0.05$, **$p < 0.01$ via model group. (For interpretation of the references to color in this figure legend, the reader is referred to the Web version of this article.)

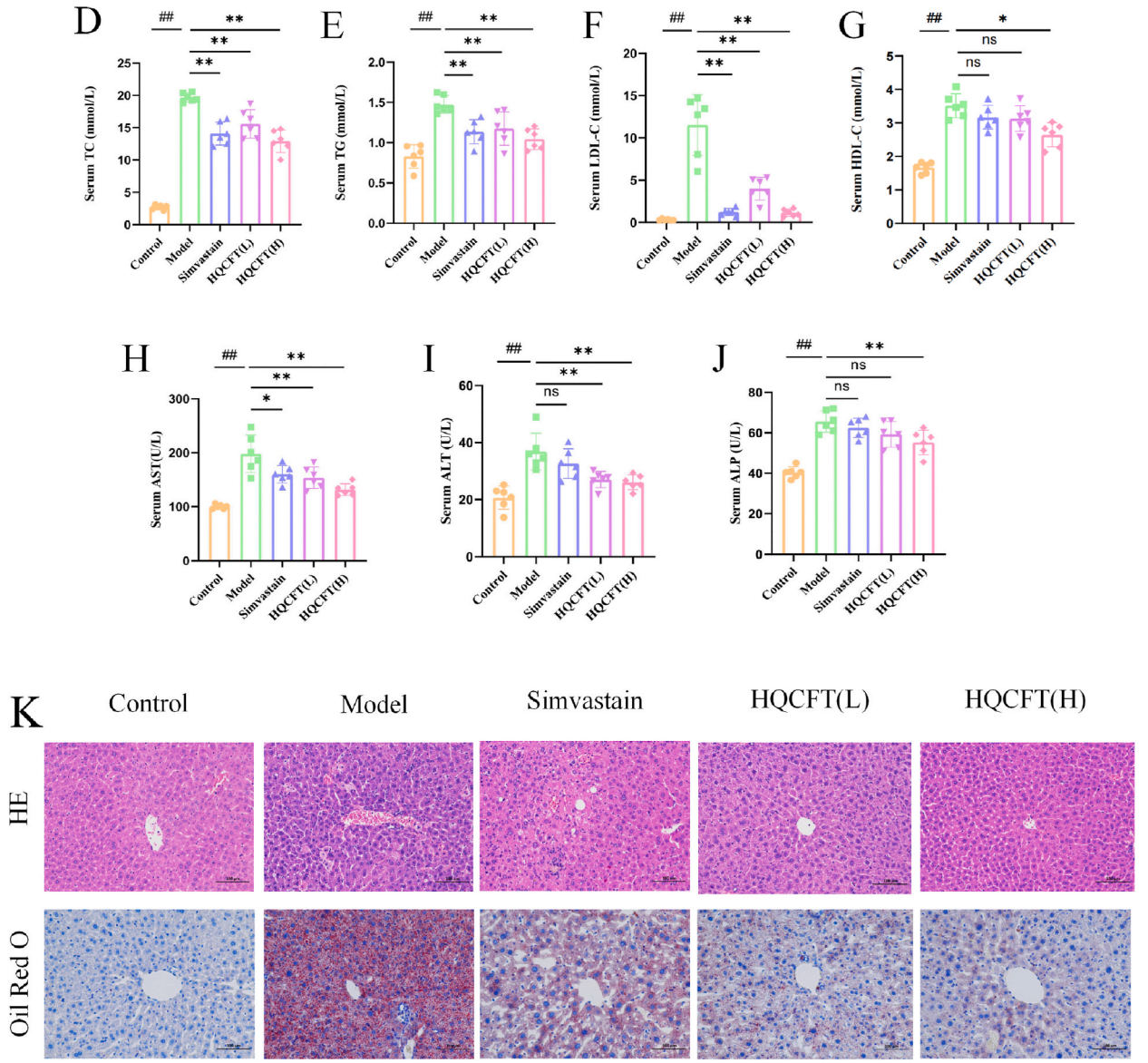

Fig. 1. (*continued*).

(#25055-1-AP), and LXRα (#14351-1-AP) antibodies were purchased from Proteintech (Wuhan, China), and goat anti-rabbit/mouse (GB25301, GB23303 1:5000) antibody was purchased from Wuhan Servicebio Technology Co., Ltd. (Wuhan, China). Methanol, acetonitrile, acetic acid, acetone and formic acid were purchased from Fisher Scientific (Fair Lawn, NJ, USA).

2.2. Animals and treatment

ApoE$^{-/-}$ mice are a classic model of atherosclerosis research at present, not only because of the spontaneous formation of atherosclerotic lesions but more importantly because their pathological and histological morphology is very similar to that of humans. Mice fed a high-fat diet are one of the commonly used animal models for the study of atherosclerosis. Male C57BL/6J wild-type mice and male ApoE$^{-/-}$ mice on a C57BL/6J background (six weeks of age, 18–20 g) were purchased from Liaoning Changsheng Biotechnology Co., Ltd. (Liaoning, China) with the license number SCXK(Liao)2020-0001. The mice were housed individually in wire cages under controlled humidity (50 ± 10 %) and temperature (25 ± 2 °C) with a light-dark cycle of 12 h. After acclimatization to a standard chow diet for 1 week, the 30 mice were divided into five groups. Wild-type C57BL/6J mice were used as the chow group and were placed on a standard chow diet for 16 weeks (n = 6). ApoE$^{-/-}$ mice with free access to a high-fat diet (D12108C: Xiaoshu Youtai Biotechnology Co., Ltd., Beijing, China) were randomly subdivided into four groups (n = 6 per group): Model group (HFD-fed mice); HQCFT(L) group: HFD-fed mice treated with low-dose HQCFT (1.95 g kg^{-1}·d^{-1}); HQCFT(H) group: HFD-fed mice treated with high-

dose HQCFT (3.90 g $kg^{-1}·d^{-1}$); Positive control group: HFD-fed mice treated with simvastatin (5 mg kg^{-1} d^{-1}). The doses used for animal intragastric administration were converted according to the human and animal equivalent dose conversion factor. Low- or high-dose HQCFT and simvastatin were administered orally to the mice by gavage once a day for 8 weeks, while the chow and HFD group mice received an equal volume of normal saline (Fig. 1A). After the experiment, all mice were killed by cervical dislocation under deep anesthesia. After dissection, the ileum tissue, liver tissue cecum content and serum were collected and stored at −80 °C for further analysis. All animal experiments were performed in accordance with the Guide for the Care and Use of Laboratory Animals by the National Institutes of Health. The protocol was approved by the Committee on the Ethics of Animal Experiments of Heilongjiang University of Chinese Medicine, China, and the approval number was 2022082102.

2.3. Biochemical assay

The whole blood was kept at room temperature for 60 min and centrifuged at 3000 rpm for 10 min, and serum samples were taken. The liver tissue was defrosted at room temperature, approximately 200 mg of the liver was cut and chopped into pieces. Precooled normal saline was added at a ratio of 1:9, ground on ice with a homogenizer for 2 min, and centrifuged at 3000 r/min for 10 min, and the supernatant was taken for use. TC, TG, LDL-C, HDL-C, AST, ALT and ALP in serum were measured using a biochemical analyzer (Reddo Life Sciences Co., LTD, China).

2.4. Histopathological assessment and immunohistochemistry staining

The aortas and livers of mice were fixed overnight with 4 % paraformaldehyde, and paraffin sections were prepared at a thickness of 4 μm, dewaxed with xylene, washed with ethanol, stained with hematoxylin-eosin, and sealed with neutral resin. The morphological changes in the mouse aorta and liver tissues were observed under an optical microscope. Liver tissues were dehydrated and successfully embedded in 15 % and 30 % sucrose to make frozen sections. Lipid deposition in the liver tissues of mice in each group was observed by oil red O staining, 75 % ethanol differentiation, hematoxylin restaining, rinsing with running water and sealing with glycerin gelatin.

For immunohistochemical analysis, mouse ileal paraffin blocks were prepared into 4 μm thick sections, dewaxed in water, antigen-repaired, blocked with nonspecific antigen, and directly incubated with primary antibody (FXR, 1:200; LXRα, 1:100) at 4 °C overnight. Drops of secondary antibody, DAB color development, hematoxylin restaining, hydrochloric acid alcohol differentiation, dehydration, transparent, neutral gum seal. Immunohistochemistry sample images were quantified using ImageJ software (version 4.2).

2.5. 16S rDNA bioinformatics analysis and statistics

Total bacterial genomic DNA was extracted from the cecal junction content of mice using a MagPure Soil DNA LQ Kit (Magan) following the manufacturer's protocol. The original sequencing data were processed by the Illumina NovaSeq platform (Thermo Fisher Scientific, USA) and agarose gel electrophoresis. Using genomic DNA as a template, PCR amplification of the bacterial 16S rRNA gene was performed using specific primers with Barcode and Takara Ex Taq hi-fi enzyme. The V3–V4 hypervariable regions of the bacterial 16S rRNA gene were amplified with primers 343F (5′-TACGGRAGGCAGCAG-3′) and 798R (5′-AGGGTATCTAATCCT-3′) using a thermocycler PCR system. Sequencing was performed on an Illumina NovaSeq 6000 with 250 bp paired-end reads. (Illumina Inc., San Diego, CA; OE Biotech Company; Shanghai, China). Using the divisive ampliCon denoising algorithm (DADA2) for depriming, quality filtering, denoising, splicing and dechimerism, high-quality read data are divided into operational taxa (operational taxonomic units, OTUs) with 97 % similarity. QIIME2 software was used for alpha and beta diversity analysis. Alpha diversity analysis (Chao1 index, Shannon index and Simpson index), beta diversity analysis (principal coordinate analysis, PCoA), community structure analysis of each group at the phylum and genus levels, species composition heatmap and other methods were used to obtain microbial-related information. The Wilcoxon rank-sum test and Kruskal–Wallis H test identified the differentially abundant taxa with $p < 0.05$.

2.6. Targeted bile acid detection

Appropriate samples were weighed and added to 100 μL of precooled methanol-water (1:1, containing internal standard CA-d4 and GCA-C13) solution, ground with a grinder (60 Hz, 2 min), and 500 μL of ice acetonitrile (containing 5 % ammonia) was added. Ultrasonic extraction was performed in an ice water bath for 20 min and left for 30 min at −20 °C. After centrifugation for 10 min (4 °C, 13000 rpm), 300 μL of supernatant was dried and redissolved in 300 μL of methanol-water (1:1, containing internal standard L-2-chlorophenylalanine and Lyso PC17:0) solution, vortexed for 30 s, ultrasonicated for 5 min, and centrifuged for 10 min (13000 rpm, 4 °C). Two hundred microliters of the upper liquid in the sample bottle was filtered by a 0.22 μm membrane and was taken for UPLC–MS/MS analysis.

The UPLC–ESI–MS/MS system (AB ExionLC, USA) equipped with a Phenomenex Kinetex C18 (internal diameter, 2.1 mm × 100 mm, 2.6 μm; FLM, China) was applied to separate 40 bile acids as previously described. A 5 μL aliquot of the sample was injected into the columns. The UPLC mobile phase consisted of solvent A (0.1 % formic acid in water) and solvent B (methanol:acetonitrile:isopropyl alcohol = 1:1:1, containing 0.1 % formic acid). The gradient duration was 12 min at a constant flow rate of 0.45 mL/min. The metabolites were eluted using a linear gradient of 20 % solvent B for 0.5 min, 20%–38 % solvent B for 0.5–1.5 min, 38%–50 % solvent B for 1.5–7.5 min, 50%–95 % solvent B for 7.5–10 min, 95 % solvent B for 10–11 min, 95%–20 % solvent B for 11–11.01 min, and 20 % solvent B for 11.01–12 min. MS analysis was conducted using an AB Sciex Qtrap 6500+ Mass Spectrometer (AB ExionLC, USA) with

electrospray ionization (ESI) in positive (5500 V) and negative modes (−4500 V). The ion source temperature and column temperature were 450 °C and 45 °C, respectively. Spray gas (Gas1) was 55 psi, and auxiliary heating gas (Gas2) was 55 psi.

2.7. Quantitative real-time PCR (RT–qPCR) analysis

Total RNA was extracted from the liver and ileum using TRIzol reagent (TAKARA, Japan). Using a Prime Script RT Reagent Kit (TAKARA, Japan), a purified 500 ng sample of total RNA from each ileal/liver sample was reverse transcribed to create cDNA templates. The qPCR primers were designed and synthesized. Then, RT–qPCR analysis was performed with Power Up SYBR Green PCR Master Mix (ABclonal, Wuhan, China). The value of the target gene was normalized to that of GAPDH. Relative expression of the measured genes was determined by the 2-ΔΔCT method. The forward and reverse sequences of the qPCR primers, which were created and synthesized, are displayed in Table 1.

2.8. Western blot analysis

Total protein was isolated from the liver by RIPA working solution (Beyotime Shanghai, China) containing 1 mM protease inhibitor and 1 mM phosphatase inhibitor. The protein concentration was determined by the Enhanced BCA Protein Kit (Beyotime Shanghai, China). Protein samples were electrophoresed at continuous voltages of 60 V for the concentration gel and 100 V for the separation gel before being transferred to a PVDF membrane. For 30 min at room temperature, the cells were blocked with TBST containing 5 % skim milk powder. The main antibody (FXR, 1:3000; LXRα, 1:5000) solution corresponding to the closed PVDF membrane was added, and the incubation period was 2 h at room temperature. After adding the secondary antibody solution and allowing it to sit for 1 h at room temperature, the membrane was exposed to ECL. GAPDH (GAPDH, 1:2000) was used as the loading control in the interim. The band density was analyzed using ImageJ software (version 4.2).

2.9. Statistical analysis

Data are shown as the mean ± SEM. Two-tailed Student's *t*-test or one-way analysis of variance (ANOVA) was conducted using SPSS 20.0 (IBM SPSS, USA). For nonparametric variables, the Wilcoxon test was used for comparisons between two groups, and the Kruskal–Wallis test was used for comparisons between three groups. $P < 0.05$ was considered statistically significant. All statistical analyses were performed using GraphPad Prism software (USA).

3. Result

3.1. HQCFT reduced atherosclerosis development

HE staining revealed a smooth and continuous intima of the aorta in the control group, with no fracture of the elastic membrane and no atherosclerotic lesions. Fibrous plaques were observed locally in the model group, with thickened vessel walls, a few cholesterol fissures surrounded by connective tissue hyperplasia and a small infiltration of foam cells, and more vascular smooth muscle cells with mild hydropic degeneration and loose and lightly stained cytoplasm. In the HQCFT group, the plaque area was significantly reduced, and its morphological structure was significantly improved compared with that of the model group, except for the mild watery degeneration of vascular smooth muscle cells and the cytoplasmic sparseness and light staining (Fig. 1C).

As shown in Fig. 1D-G, compared with the NC group, the HFD diet resulted in significantly higher serum total cholesterol (TC),

Table 1
Primer sequences for RT-qPCR analysis.

Name of primer	sequences
GAPDH	F:5′-TTTGGCATTGTGGAAGGGCTCAT-3′ R:5′-CACCAGTGGATGCAGGGATGATGT-3′
FXR	F:5′-CCTCCTCGTCTTACTATTCC-3′ R:5′-GTCACAGGCATCTCTGATAC-3′
LXRα	F:5′-AGACCAGGGAGGCAACACTT-3′ R:5′-CTTTTGTGGACGAAGCTCTG-3′
CYP7A1	F:5′-CAACGTATCATGAGACCTCCAGTC-3′ R:5′-CAGCTTCAAACATCACTCGGTAG-3′
CYP8B1	F:5′-CTGGACAAGGGTTTTGTGCC-3′ R:5′-CCCGCATCCCCTTCAAGAAT-3′
CYP27A1	F:5′-CATCCAATACACTGACCTGGG-3′ R:5′-ACCACACCAGTCACTTCCTTG-3′
ABCA1	F:5′-AGGAAACCCAATCCCAAACACTC-3′ R:5′-GAGGACACACAGGCAGGATCTTC-3′
ABCG1	F:5′-GTTCAGGAGGCCATGATGGT-3′ R:5′-CCGTCTGCCTTCATCCTTCTC-3′
HMGCR-R	F:5′-GGGCCCCACATTCACTCTT-3′ R:5′-GCCGAAGCAGCACATGATCT-3′

triglycerides (TG) and low-density lipoprotein cholesterol (LDL-C) and significantly lower serum high-density lipoprotein cholesterol (HDL-C) in ApoE$^{-/-}$ mice. In addition, both HQCFT(L) and HQCFT(H) significantly reduced TC, TG and LDL-C levels. Regarding HDL-C levels, significant differences were observed only in the high-dose group. HQCFT can regulate HDL-C to normal levels.

3.2. HQCFT for liver tissue improvement

ApoE$^{-/-}$ mice have abnormal lipid metabolism due to the functional inactivation of the apoe gene, which, together with high-fat diet feeding, results in significantly elevated lipid levels in the blood; as the liver is the main lipid-metabolizing organ, this is accompanied by significant lipid deposition in the liver. As shown in Fig. 1K, the hepatic cells in the control group were closely arranged and normal in morphology, the lobules of the liver were clearly delineated and regularly arranged, the hepatic blood sinusoids and portal areas were visible, the hepatocytes around the confluent areas and central veins were clear and intact, and there was no inflammatory cell infiltration or necrotic cells. In the liver tissue of the mice in the model group, there were primarily hepatocytes with mild steatosis, small round vacuoles in the cytoplasm, rare hepatocytes with punctate necrosis and nuclear fragmentation or lysis, and a few lymphocytes infiltrating around the local central vein. In the simvastatin group, hepatocytes were still partially visible as lesion areas, with tiny round vacuoles in the cytoplasm and multiple infiltrations of foam cells. In the HQCFT dose group, hepatocyte necrosis and inflammatory cell infiltration were reduced, but the hepatocytes in the HQCFT group showed varying degrees of mild aqueous

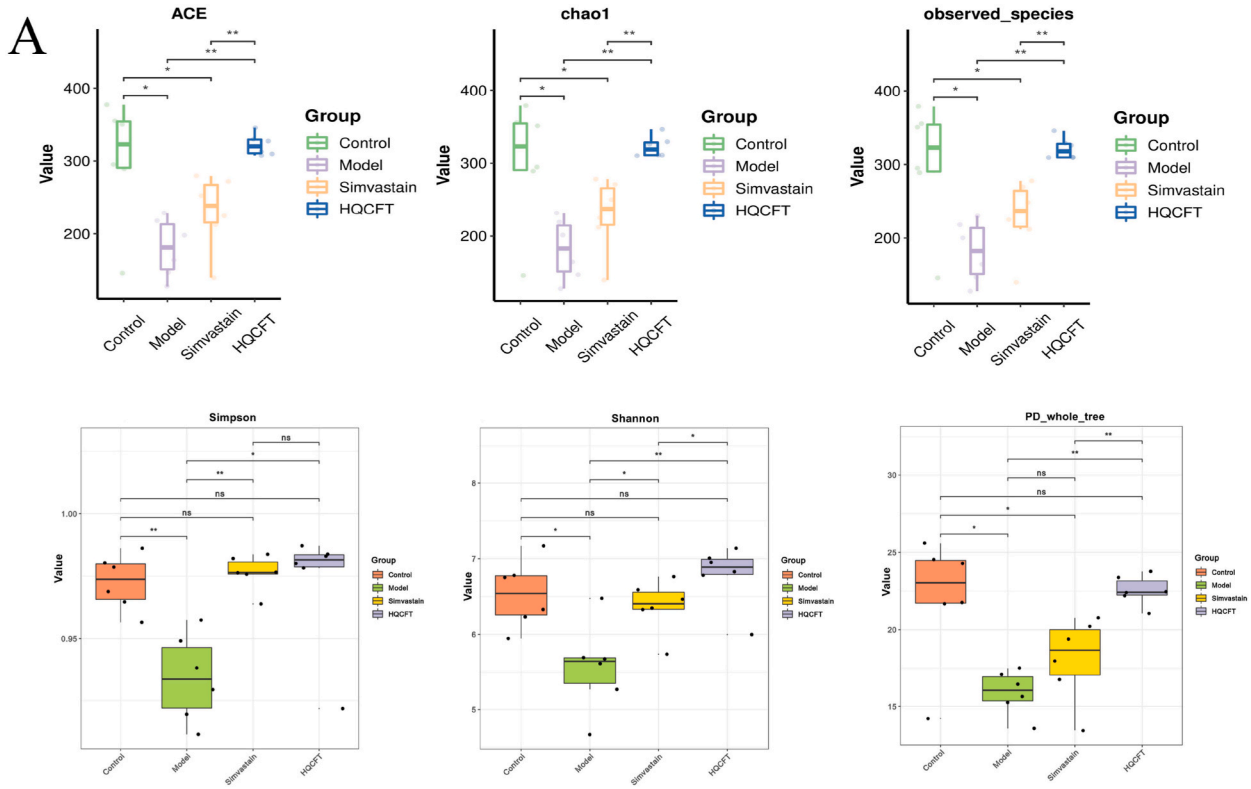

Fig. 2. HQCFT reshaped the gut microbiota in ApoE−/− mice(n = 6). (A) Alpha diversity evaluated from the ACE,Chao1 index, Observed species, Simpson,Shannon and Faith's PD index. (B) PCoA plot of Bray-curtis distance. (C)The result of hierarchical clustering tree between samples.(D) Variations in the gut microbiome at the phylum level. (E) Variations in the gut microbiome at the genus level. (F)Significantly different taxa between group analyzed by LEfSe analysis. Note:Different colors indicate different groups. The red nodes represent species with significant differences that are relatively high in abundance in the red group, the green nodes represent species with significant differences that are relatively high in abundance in the green group, and the yellow nodes represent species that are not significantly different in comparison between the two groups. Node diameter is proportional to relative abundance. Nodes of each layer represent phylum/class/order/family/genus from the inside out, and annotations of species markers of each layer represent phylum/class/order/family/genus from the inside out. The species names represented by letters in English and Chinese are shown in the legend on the right. (G)Linear discriminative analysis (LDA) score was obtained by LEfSe analysis of fecal microbial abundance. Note:The red bars represent species with relatively high abundance in the red group and the green bars represent species with relatively high abundance in the green group. The vertical coordinate is the bacterial community with large differences between groups. The horizontal coordinate uses a bar chart to visually display the logarithmic score of LDA difference analysis of the corresponding taxonomic unit, and sorts according to the score to describe the difference size of samples in different groups. (H) Relative abundance of different microbial flora at the phylum level. (I) Relative abundance of different microbial flora at the genus level. Genera with a non-parametric factorial Kruskal-Wallis (KW) sum-rank test score≤0.05, and an LDA≥2 are listed.#$p < 0.05$, ##$p < 0.01$ via the control group; *$p < 0.05$, **$p < 0.01$ via model group. (For interpretation of the references to color in this figure legend, the reader is referred to the Web version of this article.)

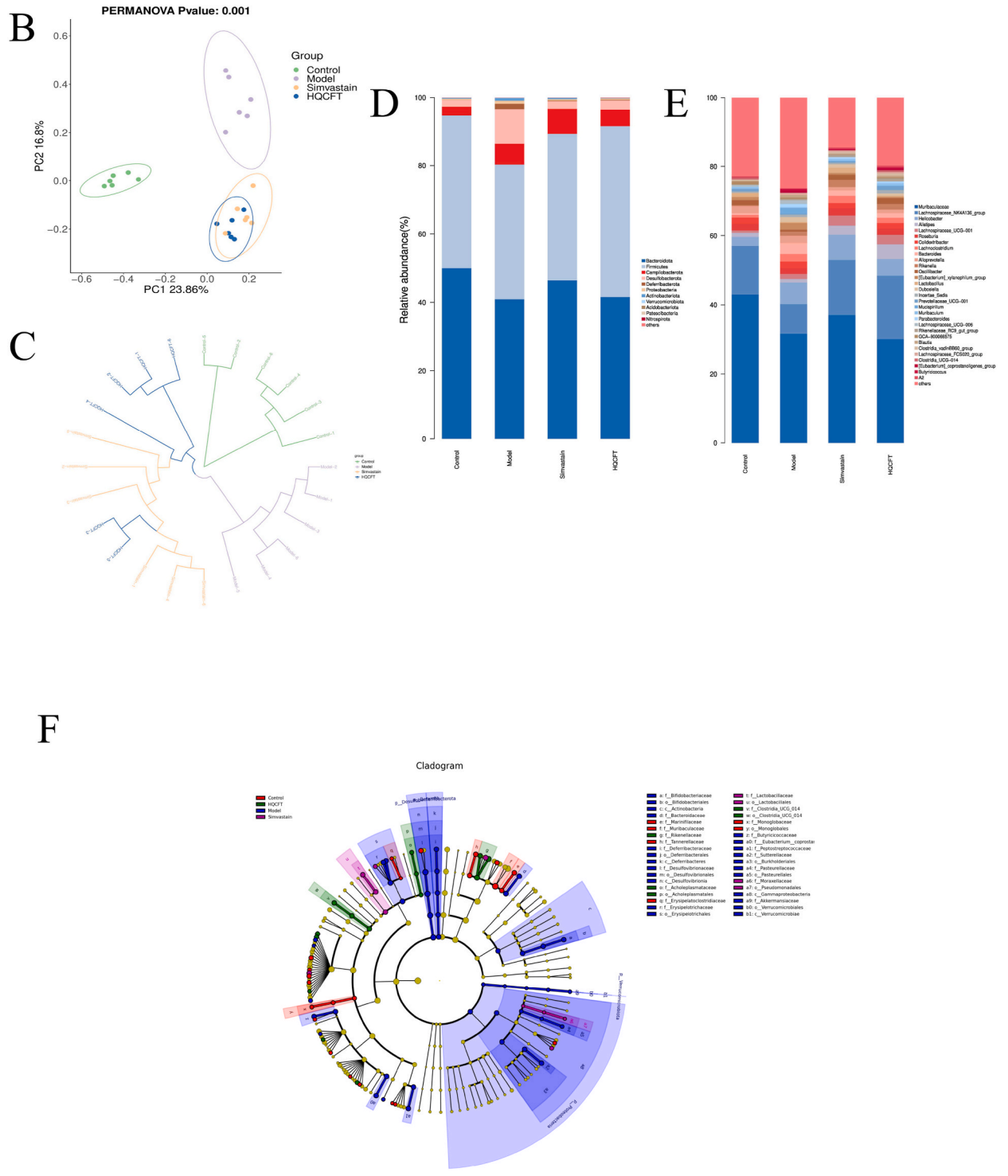

Fig. 2. (*continued*).

degeneration, cell swelling and cytoplasmic laxity. The liver tissues of mice were stained with Oil Red O. Neutral fat appeared orange–red or orange–red with blue nuclei. The model group showed a large amount of red lipid droplet accumulation compared to the control group. However, lipid accumulation in the livers of mice was gradually reduced in the HQCFT group, especially at high doses, which indicates that HQCFT intervention reversed the hepatic steatosis caused by HFD.

The serum levels of AST, ALT, and ALP were significantly increased in ApoE$^{-/-}$ mice compared to the control group of mice, and

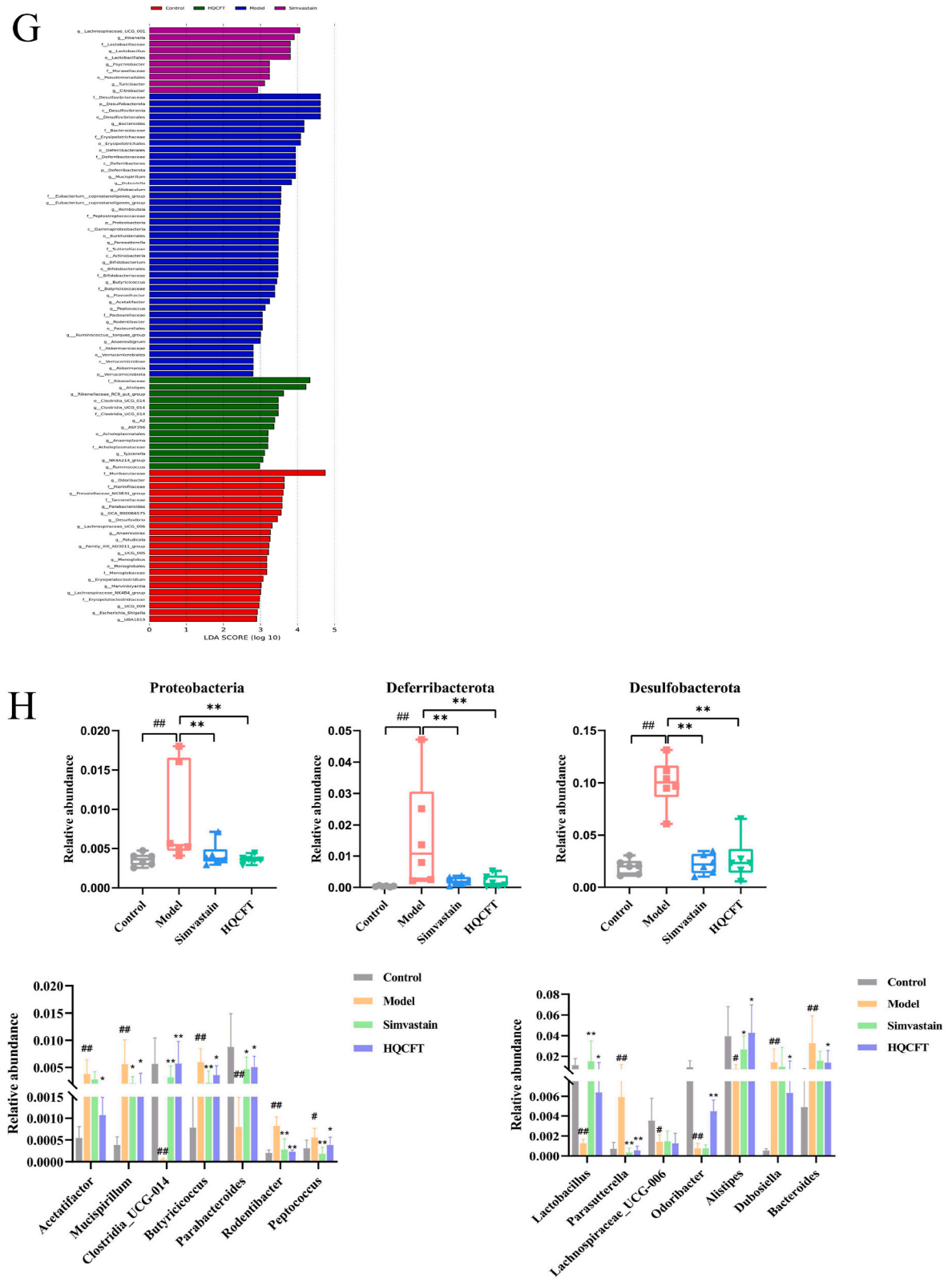

Fig. 2. (*continued*).

the ALT and AST tests suggested significant liver function impairment. The HQCFT group had significantly reduced AST, ALT and ALP levels and improved liver damage caused by a high-fat diet (Fig. 1H–J). HQCFT can regulate hepatic lipid metabolism and prevent and treat AS.

3.3. HQCFT remodels the gut microbiota in ApoE$^{-/-}$mice

To investigate the changes in the gut microbiota of ApoE−/− mice by HQCFT, we analyzed the cecum contents of each group of mice using 16SrRNA high-throughput sequencing. Significant changes in the relative species abundance and diversity of the gut microbiota of the HQCFT group. Species richness and species diversity of samples are usually expressed through the alpha diversity index. The calculated indices of community richness are Chao, ACE and observed species, and the higher the value is, the higher the richness and diversity of the community. A significance test of the α-diversity indices of the two groups was carried out, and if $P < 0.05$, the diversity and richness of the communities were considered different between groups. As shown in Fig. 2A, the results showed that the Chao1, ACE, and observed species indices decreased between the control and model groups, and there was a significant difference, indicating that the abundance of gut microbiota was altered after HFD feeding, and the abundance of flora was significantly higher in mice after HQCFT intervention. Compared with the control group, the Shannon and Simpson indices were reduced, and the colony diversity was lower in the model group. In contrast, the Shannon and Simpson indices were significantly higher in the HQCFT group. Taking Faith's PD index based on evolutionary diversity, the higher the number of species, the greater the value. Compared to normal mice, HFD decreases their species number, and after HQCFT intervention, the PD index is adjusted back, and the number of species increases.

Principal coordinate analysis (PCoA), based on the Bray–Curtis distance matrix algorithm, was used to demonstrate differences in colony composition between samples. PCoA allows observation of the degree of aggregation and dispersion between groups of samples. The higher the similarity in species composition structure between samples, the more aggregated they are in the graph, and conversely, the lower the similarity between samples, the more distant the linear distance. The PCoA results showed that the gut microbiota of the groups were significantly different and that the groups were well differentiated (Fig. 2B). The control group, model group and HQGFT had a large matrix distance between the three groups, suggesting a significant difference in colony structure between the three groups. Similarly, systematic clustering tree analysis showed (Fig. 2C) that the HQCFT group was closer to the control group than the model group. Adonis test analysis yielded $R2 = 0.44687$, $p = 0.001$, indicating that the differences were significant and that the HFD and HQCFT interventions could alter the colony structure of the cecum contents.

We analyzed the mouse gut microbiota at the phylum and genus levels (Fig. 2D and E). The four groups were found to be mainly composed of *Firmicutes, Bacteroidota*, *Proteobacteria*, *Actinobacteriota*, *Desulfobacterota* and *Deferribacteres*. The relative abundance at the level of microbial genera was further investigated. The main genera in the mouse gut microbiota include *Muribaculaceae*, *Lachnospiraceae_NK4A136_group*, *Helicobacter*, *Alistipes*, *Colidexibacter*, *Bacteroides* and *Lactobacillus*.

Linear discriminant analysis effect size (LEfSe) finds species that differ significantly in abundance between groups. The gut microbiota of the four experimental groups were first analyzed using the LEfSe method, and significant differences were found in the gut microbiota composition between the groups (Fig. 2F). The representative gut bacteria of each group can be seen in the cladogram. LDA effect sizes and P values were obtained using LEfSe analysis, and marker species that differed significantly between groups were screened for LDA >2 and $P < 0.05$ (Fig. 2G). At the phylum level, a comparative analysis of the groups revealed that *Desulfobacterota*, *Deferribacterota*, and *Proteobacteria* were relatively more abundant in the gut microbiota of the Mod group of mice, while at the genus level, *Bacteroides*, *Dubosiella, Muribaculum*, *Roseburia*, *Allobaculum*, *Parabacteroides*, *Parasutterella*, *Butyricicoccus*, *Flavonifractor*, and *Anaerostignum* were relatively more abundant at the genus level. The HQCFT group, on the other hand, showed higher relative abundances of *Alistipes*, *Rodentibacter*, *Acetatifactor*, *Peptococcus* and *Anaeroplasma* at the genus level. High-fat diets cause changes in the body's intestinal flora, with significant increases in the concentrations of *Desulfobacterota*, *Deferribacterota* and *Proteobacteria* at the gastrointestinal level, which contain many pathogenic microorganisms (such as *Helicobacter pylori* and *Salmonella*). As shown in Fig. 2H, HFD stimulated ApoE$^{-/-}$ mice to significantly increase the relative abundance of *Proteobacteria*, disrupting the equilibrium of the gut microbiota, while HQCFT significantly alleviated the increase in the relative abundance of *Proteobacteria* in AS mice. In addition, HQCFT significantly reduced the relative abundance of *Desulfobacterota* and *Deferribacterota*. The above results suggest that HQCFT can increase the abundance of beneficial bacteria and decrease the harmful bacteria associated with AS. In comparison, the detection at the genus level revealed a significant increase in the relative abundance of *Bacteroides*, *Acetatifactor*, *Parasutterella*, *Mucispirillum*, *Butyricicoccus*, *Parabacteroides* and *Rodentibacter*. The relative abundances of *Clostridia_UCG-014*, *Lactobacillus*, *Lachnospiraceae_UCG-006*, and *Alistipes* significantly decreased. The results indicated that HQCFT could significantly regulate the structure and colony abundance of intestinal flora in ApoE$^{-/-}$ mice (Fig. 2I).

3.4. HQCFT treatment improved BA metabolism

AS can be induced by long-term high-fat and high-cholesterol food-feeding conditions. The mechanism may be that mice cannot excrete excess cholesterol as bile acids through the intestine promptly, and the abnormal metabolic pathway of cholesterol to bile acids can lead to hypercholesterolemia, which is then involved in the development of AS. To determine the effect of HQCFT on BAs, we used a targeted metabolomics approach based on UPLC-ESI-MS/MS technology to determine and quantify 40 BAs in the intestinal contents of mice. Our experimental results found significant differences in the levels of 14 bile acid metabolites (Fig. 3A). Ursodeoxycholic acid (UDCA) and hyocholic acid(HCA) are for primary BAs. For secondary BAs, lithocholic acid(LCA), deoxycholic acid(DCA), hyodeoxycholic acid(HDCA), taurodeoxycholic acid(TDCA), taurolithocholic acid(TLCA), glycodeoxycholic acid(GDCA); this reveals that the

metabolism of BAs is indeed impaired in AS mice, and that HQCFT can effectively regulate the levels of these bile acids to inhibit the development of atherosclerosis by regulating bile acid metabolism and alleviating liver fat accumulation.

3.5. Spearman correlation analysis of gut microbiota and BAs

We constructed a heatmap indicating the correlation between gut microbiota levels and bile acid metabolites in mice at the genus level. Changes in the number and composition of gut microbiota also affect bile acid composition. Additionally, the gut microbiota is associated with regulating hepatic bile acid synthesis and can activate bile acid-related signaling pathways to regulate bile acid metabolism.

As shown in Fig. 3B, the results showed multiple strong correlations between the gut microbiota and metabolites ($P < 0.01$ and $|r| > 0.6$). For example, *Rodentibacter*, *Parasutterella*, *Mucispirillum*, *and Butyricicoccushas* were strongly correlated with most of BAs, especially LCA,DCA,UDCA, GLCA,TLCA and GDCA($P < 0.01$ and $|r| > 0.6$). In particular, *Odoribacter* was negatively correlated with TLCA, DCA, LCA. It is worth noting that *Parabacteroides* is negatively correlated with the content of most bile acids. In conclusion, HQCFT intervention was effective in restoring HFD-induced disorders of lipid and BA metabolism in ApoE$^{-/-}$ mice, mainly by reducing LCA, DCA, UDCA, GLCA, TLCA and GDCA, which was mainly attributed to the improvement of gut microbiota.

3.6. HQCFT changes BA recirculation partly by regulating BA-synthesizing initiating enzymes and FXR-LXR signaling in ApoE−/−mice

BA homeostasis is tightly regulated by the intestine-hepatic cycle. In addition to the maintenance of BA homeostasis, recent studies have revealed that the BA-Farnesoid X receptor (FXR) axis also plays an important role in metabolic diseases. In the liver, FXR activation induces small heterodimer partner (SHP), which inhibits the expression of CYP7A1 and CYP8B1, the rate-limiting enzymes for bile acid synthesis, and affects BA transport. The expression of FXR in the liver tissues of ApoE$^{-/-}$ mice was significantly higher, and the mRNA levels of CYP7A1, CYP8B1, and CYP27A1 were significantly lower, both at the mRNA level and at the protein level, compared with those of the control mice(Fig. 4A). However, HQCFT had an upregulatory effect on the hepatic bile acid synthesis genes CYP8B1 and CYP27A1, while the mRNA level of CYP7A1 had no significant effect. HQCFT inhibited FXR and increased the expression of CYP7A1, increasing the positive cycle of BA synthesis and clearance, accelerating the clearance of cholesterol by hepatic bile acid metabolism and alleviating cholesterol accumulation.

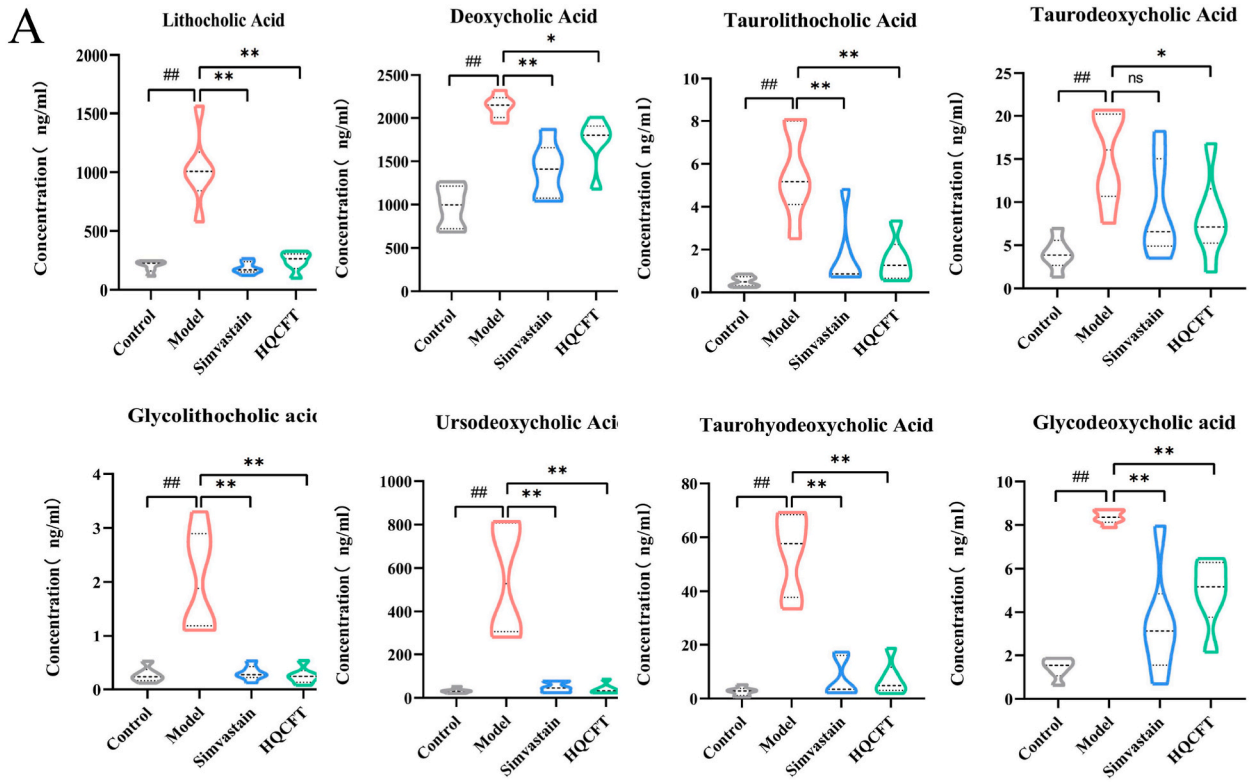

Fig. 3. HQCFT improves Apoe$^{-/-}$ mice microbial BAs dysmetabolism(n = 6).(A) Absolute quantification of different BAs in the feces of mice(n = 6). (B) Spearman's correlation analysis between the identified bacterial species and BAs. Data were expressed as mean ± SEM,and the statistically significant difference was analyzed by one-way ANOVA followed by Dunnett's multiple comparison tests. #$p < 0.05$, ##$p < 0.01$ via the control group; *$p < 0.05$, **$p < 0.01$ via model group.

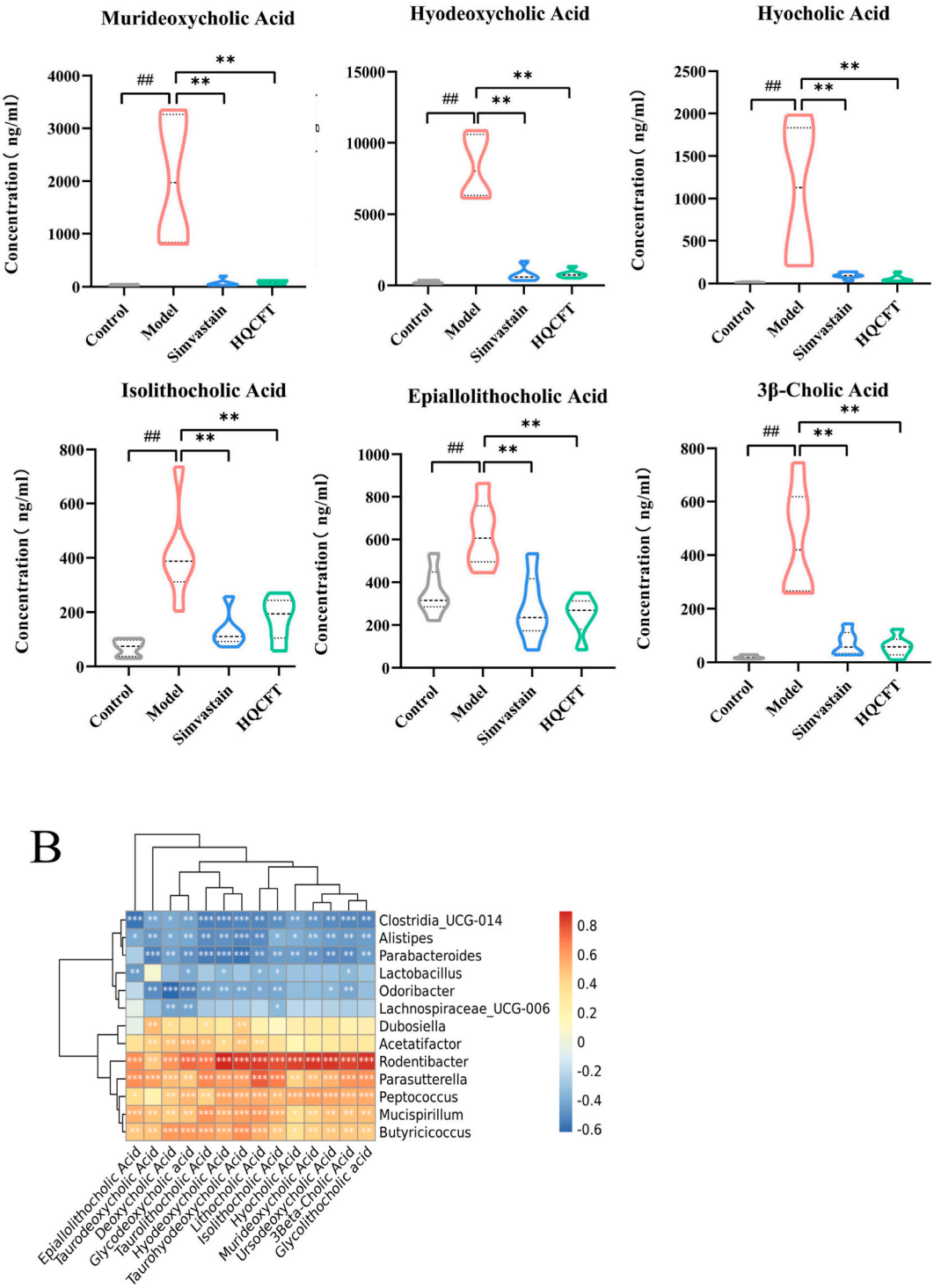

Fig. 3. (*continued*).

LXRα, ABCA1, and ABCG1 mRNA expression was decreased in the liver tissues of ApoE$^{-/-}$ mice, and there was no meaningful change in HMGCR. Compared with the mod group, LXRα, ABCA1, and ABCG1 mRNA expression was increased in liver tissues of HQCFT group mice. Thus, the LXRα-ABCA1 pathway is a key pathway in cholesterol metabolism, and promoting the expression of this signaling pathway can mediate cholesterol metabolism and reduce hepatic lipid deposition and inflammatory responses.

In addition to the liver, the intestine is an organ with high FXR expression and bile acid content(Fig. 4BC). In the ileum, FXR plays a

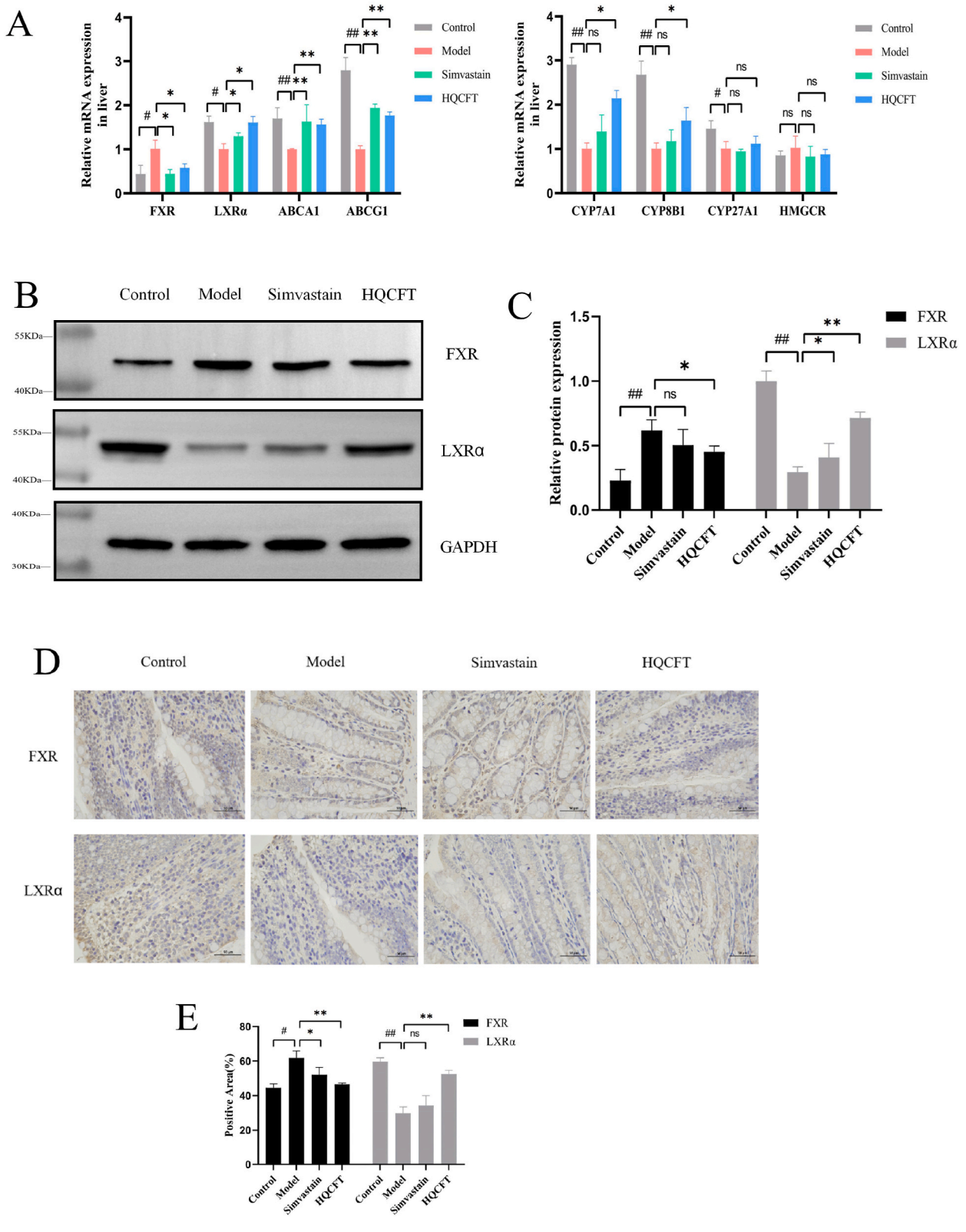

(caption on next page)

Fig. 4. (A)The mRNA expression of major genes involved in bile acid synthesis in the liver(FXR,LXRα,ABCA1,ABCG1,HMGCR,CYP7A1,CYP8B1, CYP27A1). (B)Western blots of FXR and LXRα in the liver tissue. (C)Quantification of each western blotting band. (D)IHC staining of FXR and LXRα in the ileum tissue (scale bar, 50 μm). (E)Quantification of Positive Area. The mRNA expression and protein expression were normalized to GAPDH. Data were expressed as mean ± SEM,and the statistically significant difference was analyzed by one-way ANOVA followed by Dunnett's multiple comparison tests. #p < 0.05, ##p < 0.01 via the control group; *p < 0.05, **p < 0.01 via model group.

major role in bile acid reabsorption by regulating the expression of bile acid transport proteins. In addition, immunohistochemical results showed that a high-fat diet induced an increase in FXR in the ileum, which presumably overactivated FXR in the intestine and inhibited the transcriptional level of hepatic CYP7A1, thereby reducing cholesterol metabolism, causing cholesterol accumulation and triggering AS. HQCFT intervention significantly downregulated FXR and upregulated LXRα expression, which suggests that HQCFT controls cholesterol metabolism and its conversion to bile acids by regulating FXR and LXRα activity, which in turn regulates the effects of bile acid synthesis and reabsorption(Fig. 4DE). Based on these results, HQCFT promotes the expression of CYP7A1, accelerates cholesterol metabolism and bile acid synthesis, and should increase intestinal bile acid levels; the opposite was detected for bile acid levels in feces.

4. Discussion

Atherosclerosis is a fibrositis lesion that forms on the inner walls of arteries and is the primary pathological basis for cardiovascular diseases such as ischemic heart disease and ischemic stroke [17]. It has been observed that gut microbiota structure and intestinal permeability are closely related to AS and its risk factors [18]. A decrease in the number of beneficial bacteria and an increase in the number of harmful bacteria in the intestine can lead to damage to the intestinal barrier and changes in substances such as lipopolysaccharide (LPS), short-chain fatty acids (SCFAs), bile acids (BAs) and trimethylamine oxide (TMAO), which can lead to more harmful substances entering the circulatory system, causing inflammatory reactions and oxidative stress and affecting the progression of AS [19,20]. Gut microbiota disorders can increase the number and size of plaques in AS model mice, and effective treatment can be used to remove commensal bacteria from the gut to improve the pathological state of the organism [21]. In addition, BAs and gut microbiota can modulate each other to further modify bile acid signaling, which can also impact host metabolism. The direct cause of AS is impaired cholesterol metabolism and a chronic inflammatory response; therefore, abnormal bile acid metabolism is closely related to the development of AS [22]. Studies have shown that long-term feeding of high-fat and high-cholesterol foods causes excess cholesterol in mice, which is unable to be converted into BAs in a timely manner, resulting in hypercholesterolemia [23]. Changes in the number and composition of the gut microbiota also affect the composition of BAs; at the same time, the gut microbiota is also involved in regulating the synthesis of BAs in the liver and can activate BA-related signaling pathways to regulate BA metabolism [24]. Since the gut microbiota is significantly altered in AS and related metabolic disorders, and BAs can play a signaling role in glucolipid metabolism, new preventive and therapeutic strategies can be proposed by modifying gut microbiota alterations. Therefore, studying the interaction between BAs and the gut microbiota as well as the altered signaling of BAs may provide new therapeutic strategies for AS and its associated metabolic disorders.

Therefore, in this project we explored the protective effects and specific mechanisms of action of HQCFT on ApoE$^{-/-}$ mice from gut microbiota-BA interactions. Combined with the sequencing results of gut bacteria, changes in BA profiles were measured using targeted metabolomics for gut microbiota-BA association analysis to investigate whether AS is correlated with BA metabolism and gut bacterial dysbiosis and whether HQCFT can reshape the structure of the gut microbiota and improve BA metabolism for the treatment of AS. Our results showed that HQCFT significantly reduced the plaque area and collagen deposition in the aortic plaque-vulnerable areas of ApoE$^{-/-}$ mice and reduced serum TG, TC, LDL and HDL levels in ApoE$^{-/-}$ mice, and the high-dose group was superior to the low-dose group. It is suggested that HQCFT may control AS plaque formation by improving dyslipidemia. In addition, the onset of AS is often accompanied by substantial damage to hepatocytes and dysfunction of hepatic excretion, resulting in reduced hepatic lipid metabolism and abnormal liver function. Our experimental results showed that after HFD feeding, ApoE$^{-/-}$ mice in the model group had dyslipidemia, significant hepatocyte steatosis, significant hepatic lipid deposition, and significantly increased ALT, AST, and ALP levels. After HQCFT intervention, the degree of hepatocyte steatosis and lipid deposition was reduced, confirming that HQCFT could regulate blood lipid levels, improve liver lipid deposition and significantly reduce liver function damage.

In addition, the gut microbiota plays a key role in lipid metabolism and disorders of lipid metabolism are often accompanied by adverse changes in the gut microbiota [25]. When the body's lipid metabolism is abnormal, it usually affects the number and distribution of gut microbiota, and on the contrary, disorders of gut microbiota can further aggravate the abnormal lipid metabolism [26]. A high-fat and high-sugar diet induces dysfunction of the gut microbiota, disrupting intestinal barrier function and stimulating an inflammatory response in intestinal tissues [27]. Analysis by 16S rDNA sequencing revealed that the gut microbiota of each group of mice consisted mainly of *Firmicutes*, *Bacteroidota*, *Proteobacteria*, *Actinobacteriota*, *Desulfobacterota*, *Deferribacteres*; at the genus level, this is mainly *Acetatifactor*, *Mucispirillum*, *Butyricicoccus*, *Parabacteroides*, *Rodentibacter*, *Lactobacillus*, *Parasutterella* and *Bacteroides*, *Odoribacter*, *Alistipes*, *Dubosiella*, etc. It is evident that HFD reduces the abundance of beneficial intestinal bacteria and increases the abundance of harmful bacteria, resulting in dysbiosis, immune dysfunction and exacerbation of the disease process. Bacteroides and Lactobacillus are recognized as BSH-active bacteria, and elevated BSH activity can promote the hydrolysis of BAs in the gut and increase the excretion of BAs. HQCFT intervention significantly reversed the HFD-induced alterations in the above gut microbiota at both the gate and genus levels and regulated the abundance of Bacteroides and Lactobacillus associated with BSH. Therefore, we speculated that HQCFT could reduce the abundance of pathogenic bacteria, increase the abundance of probiotics, and reshape the structure of

intestinal flora, thus playing a role in the prevention and treatment of AS.

The gut microbiota and BAs are important in host metabolism, as BAs are the products of cholesterol metabolism in the liver. The classical pathway is the production of cholic Acid (CA) by CYP7A1 and CYP8B1, which accounts for approximately 75 % of the total BAs in the body, while the alternative pathway is the production of chenodeoxycholic Acid (CDCA) by the action of CYP27A1 and CYP7B1. The primary BAs synthesized in the liver are mainly CA and CDCA, with CA binding to glycine or taurine to produce glycocholic Acid (GCA) and taurocholic Acid (TCA), and CDCA binding to glycine or taurine to produce glycochenodeoxycholic acid (GCDCA) and taurochenodesoxycholic Acid (TCDCA) [28]. Primary BAs are synthesized in the liver and stored in the gallbladder, and when stimulated by fatty foods, they are transported by the bile ducts to the duodenum. Over 95 % of BAs are reabsorbed at the end of the ileum via the portal vein to the liver, completing the enterohepatic cycle [29]. In the intestine, specific intestinal bacteria can produce bile salt hydrolase (BSH), which uncouples bile acids, and intestinal bacteria can convert CA and CDCA into secondary BAs (e.g., DCA, LCA, UDCA), thereby reducing the toxic effects of hydrophobic BAs on the liver [30]. Secondary BAs can be recoupled after intestinal reabsorption into the liver to further regulate host metabolism and gut microbial composition [31]. Altering the composition and size of the pool of BAs by modulating gut microbiota provides a potential therapeutic and preventive strategy for preventing the emergence of AS.

In our experimental results, UDCA, TUDCA, and HCA were increased in the feces of mice in the Mod group compared to the control, probably because of the compensatory increase caused by a high cholesterol and high-fat diet, which increases the catabolic absorption of lipids and affects the digestion and absorption of some nutrients. In contrast, HQCFT intervention significantly reduced UDCA, TUDCA and HCA levels, mainly by regulating primary BAs in the feces to regulate lipid metabolism in AS mice. LCA, a common hydrophobic BA, is a secondary metabolite of intestinal microorganisms that can damage hepatocytes by destroying the integrity of cell membranes, promoting the production of reactive oxygen species and oxidatively modifying lipids, proteins and nucleic acids through the descaling of cell membrane lipids [32]. It has been observed that HFD induces a high secretion of bile, which can significantly increase the level of secondary BAs in the intestinal feces, especially DCA. Some researchers have found that DCA levels in the feces of HFD animals were nearly 10-fold higher than those in a normal diet and that intestinal defenses were impaired [33]. The results of the experiment revealed that the free BAs LCA, DCA, HDCA and the bound BAs GLCA, GDCA, TLCA, and THDCA were significantly increased in the feces of ApoE$^{-/-}$ mice, probably because the conversion between free and bound BAs was impaired, resulting in the inability to excrete BAs efficiently and leading to further development of atherosclerosis. HQCFT improves BA metabolism by intervening in BA composition and mass concentration changes. Therefore, we analyzed the correlation between gut bacteria and BAs to look for possible changes in bacteria and metabolite populations and to reveal possible relationships.

At the genus level, HFD increased the abundance of enteropathogenic and conditionally pathogenic bacteria such as *Parasutterella* and *Rodentibacter* in ApoE$^{-/-}$ mouse intestinal bacteria. *Parasutterella*, a genus of Proteus beta, has been defined as a member of the healthy fecal core microbiome in the human gastrointestinal tract (GIT) [34], with potential roles in BA maintenance and cholesterol metabolism [35]. Other studies have shown that increased *Parasutterella* abundance correlates with ecological dysregulation or reduced gut microbiota diversity [36]. Our experiments revealed that HQCFT significantly reduced the relative abundance of *Parasutterella* and maintained BA metabolism. After Pearson correlation analysis,we found that *Parasutterella* was positively correlated with LCA, TUDCA, TLCA, and GLCA, suggesting that *Parasutterella* is associated with the production of secondary BAs and that HQCFT may regulate the content of secondary BAs by regulating the abundance of *Parasutterella*. In some cases, *Rodentibacter* has been reported to act as a pathogenic agent, even as a major pathogen [37]. The abundance of *Rodentibacter* is positively correlated with inflammatory cytokines and can exacerbate the inflammatory response of the respiratory system by affecting the immune function of Th1 and Th2 cells, thereby increasing the damage caused by the disease and even increasing the mortality rate [38]. Our experiments revealed that the relative abundance of *Rodentibacter* was significantly increased in the ApoE$^{-/-}$ mice, suggesting that *Rodentibacter* may contribute to the developmental progression of AS. Correlation analysis revealed a positive correlation between *Rodentibacter* and most BAs, such as HCA, HDCA, DCA, LCA, UDCA, THDCA, GDCA, TLCA and GLCA, suggesting that HQCFT regulates cholesterol levels by reducing the abundance of *Rodentibacter* and restoring BA homeostasis and intestinal permeability.

This result was also confirmed by a study in which *Parabacteroides* had a strong ability to convert primary BAs into secondary BAs. *Parabacteroides* controlled weight gain, reduced hyperglycemia and hyperlipidemia, improved hepatic steatosis in mice, and enhanced hepatic metabolic dysfunction by affecting the succinate pathway and secondary BA metabolism [39]. In our experiment, it was found that HQCFT can significantly improve the relative abundance of *Parabacteroides*. These results indicated that *Parabacteroides* could be used to improve lipid levels and liver metabolic function. *Odoribacter* is primarily a succinate-consuming bacterium that is associated with intestinal succinate metabolism [40]. Our experimental results found a negative correlation between *Odoribacter* and DCA. It has been hypothesized that HQCFT regulates intestinal succinate metabolism and avoids local oxidative stress in the intestine due to AS by increasing the abundance of *Odoribacter* and decreasing DCA content. *Butyricoccus* is a beneficial bacterium that suppresses inflammatory bowel disease. In large quantities, butyrate maintains intestinal immunity, exerts anti-inflammatory properties and supports the maturation of the immune system, acting as an important bridge to host metabolism [41]. However, the abundance of the short-chain fatty acid-producing bacteria *Butyricicoccus* was detected significantly higher in the model group of mice than in the control group, possibly due to a compensatory elevation induced by high lipids, and the excess bacteria may inactivate their own gut microbiota, thereby inhibiting the gut from repairing itself after suffering damage. A correlation between *Butyricoccus* and DCA, TUDCA, GDCA, and TLCA was also found, but the relationships among them have yet to be verified. Our results found that high lipids increased the abundance of *Mucispirillum* in the intestinal bacteria of ApoE$^{-/-}$ mice. When inflammation occurs in the gut, substances such as reactive oxygen species increase, and this genus has several systems for scavenging oxygen and reactive oxygen species and can adapt to the oxidative stress environment of the mucus layer, which may explain its persistence and increased relative abundance in the gut with inflammation [42]. Our results also confirm this conclusion. Moreover, correlation analysis revealed that *Mucispirillum*

was negatively correlated with LCA and TLCA. In contrast, HQCFT could prevent hepatic steatosis and inflammatory changes caused by AS by reducing *Mucispirillum* abundance.

Most diseases associated with disorders of BA metabolism are caused by a decrease in the activity or absence of key enzymes involved in the synthesis and metabolism of BAs, a decrease in the synthesis of BAs due to damage to hepatocytes and the accumulation of large amounts of cholesterol and metabolites in the body [43,44]. The liver and intestine are the main sites of synthesis and dissociation of bound BAs, and the "intestine-liver" dialog is an essential process that regulates the metabolism of BAs in the body. Among the BA components, CDCA, CA, DCA, LCA, TCA and TCDCA are FXR agonists [45]. BAs are endogenous ligands for farnesoid X receptor (FXR), which regulates the activity of genes related to BA synthesis, transport, binding and excretion [46]. Under normal physiological conditions, hepatic FXR activity regulates BA and BA levels in the intestine while limiting BA accumulation in the liver. Intestinal FXR maintains the return of BAs to the portal vein and controls the reabsorption of BAs into enterocytes, thus limiting intracellular BA levels during the synthesis, excretion and uptake chain. The study found that the microbiome regulates bile acid metabolism and synthesis in an FXR-dependent manner [46,47]. Our results showed that FXR expression was increased in both the liver and ileum of ApoE$^{-/-}$ mice, suggesting that a HFD may cause an excessive content of bile acids for cholesterol metabolism in the body, requiring more FXR to bind to it. Activation of FXR can indirectly inhibit the expression of the CYP7A1 and CYP8B1 genes and inhibit the synthesis pathway of cholesterol and bile acid.

To investigate whether HQCF regulation of bile acid metabolism and synthesis is dependent on the FXR signaling pathway, we examined the relative expression levels of some key genes that may be associated with regulating the metabolism of BAs. CYP7A1, CYP8B1, and CYP27A1 are all implicated in regulating the BA synthesis pathway. We concluded that although the mRNA expression levels of CYP7A1, CYP8B1, and CYP27A1 were all inhibited, the mRNA levels of CYP7A1 and CYP8B1 were significantly increased in the HQCFT group, whereas the mRNA of CYP27A1 was not affected. HQCFT could promote the downstream expression of CYP7A1 and CYP8B1 by downregulating hepatic FXR expression.

Liver X receptor α(LXRα) is a key sterol-sensitive transcription factor in the reverse cholesterol transport pathway. Its expression is

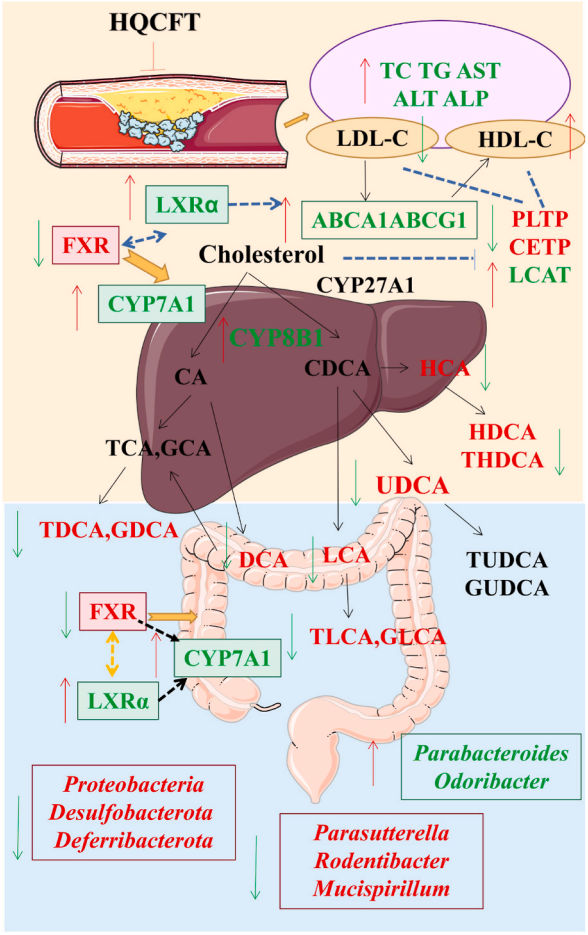

Fig. 5. Proposed mechanism for HQCF to treat AS. Red color: the increased BAs, gut microbiome and protein of model; Green color: the decreased BAs, gut microbiome and protein of model; ↓having signification decreased after HQCFT treatment; ↑ having signification increased after HQCFT treatment. (For interpretation of the references to color in this figure legend, the reader is referred to the Web version of this article.)

highly correlated with hepatic fat deposition and plays a key role in the transcriptional regulation of cholesterol homeostasis [48]. LXRα deficiency leads to peripheral cholesterol accumulation and hepatic lipid deposition. However, high LXRα expression reduces high-fat diet-induced liver inflammation [49]. Activation of LXR can promote cholesterol metabolism by inducing CYP7A1 through the classical pathway and inducing ATP-binding cassette transporter A1/G1 (ABCA1/G1), which stimulates cholesterol reversal transport and reduces cholesterol overload in vivo [50]. When ABCA1 expression is absent or dysfunctional in mammalian models, intracellular ApoA1 is degraded because it is unable to bind cholesterol, leading to lower plasma HDL-C levels and cholesterol deposition in the vessel wall [51]. We found that ABCA1 mRNA and protein expression were reduced in the model group, ABCA1 expression increased, increasing ApoA1 binding to cholesterol, inhibiting the degradation of ApoA1 in the liver on the one hand, and achieving the effect of lowering blood lipids on the other. ABCG1, as an important membrane protein for maintaining intracellular ABCG1, an important membrane protein for maintaining intracellular cholesterol and phospholipid homeostasis, promotes HDL-2, HDL-3 and HDL binding to apolipoproteins and acts synergistically with ABCA1 to avoid excessive accumulation of cholesterol in hepatocytes that may cause liver injury [52]. However, HQCFT upregulated LXRα protein expression levels and activated hepatic ABCA1 and ABCG1 transcript levels, thereby allowing cholesterol to be transferred from a plaque in the thoracic aorta to the liver and metabolized out of the body. HQCFT reduced ileal BAs. Therefore, inhibiting the activity of the enterohepatic FXR/LXRα axis accelerates CYP7A1-and CYP8B1-mediated cholesterol catabolism in the liver and thus promotes the synthesis of hepatic BAs. This study found that targeted gut microbiota treatment could regulate the synthesis of hepatic BAs by affecting the enterohepatic FXR/LXRα axis. Thus, precise regulation of FXR levels can play a crucial role in maintaining bile acid homeostasis in the enterohepatic circulation(Fig. 5).

5. Conclusions

The metabolism of BAs by the gut microbiota and the regulation of organismal metabolism by BAs are two key factors in the establishment of the gut microbiota-Bas-host metabolic axis. The changing gut microbiota composition and dynamic bile acid pools also provide new strategies for the treatment of AS. Our study found that HQCFT reduced TC, TG, LDL-C, ASL, and ALT levels and increased HDC-C levels. Thus, we speculate that HQCFT may improve the structure and abundance of gut microbiota and regulate the bile acid content, decrease FXR agonists (CDCA, LCA, DCA) in BA fractions, inhibit intestinal FXR, and increase BA efflux. HQCFT also increased the expression of LXRα, increased the levels of hepatic CYP7A1 and CYP8B1, promoted the synthesis of more BAs in the liver to enter the intestine, and maintained the balance of cholesterol metabolism. The mechanism of HQCFT for AS treatment was elucidated from the perspective of the gut microbiota-BAs-FXR axis, which further enriched the mechanism of HQCFT's anti-atherosclerotic action. However, our study also has some limitations. In the future, we must thoroughly explore a specific genus of bacteria regulated by HQCFT to verify the genetic function of the genus and determine whether it directly affects the metabolism of BAs.

Data availability statement

Data associated with this study has been deposited at NCBI under the accession number PRJNA924031. The original contributions presented in the research are included in the article/supplementary material, and further queries can be directed to the corresponding authors.

CRediT authorship contribution statement

Jiaqi Fu: Writing – original draft, Visualization, Methodology, Formal analysis. **Yuqin Liang:** Methodology, Formal analysis. **Yunhe Shi:** Software, Formal analysis. **Donghua Yu:** Software, Formal analysis. **Yu Wang:** Visualization, Software. **Pingping Chen:** Validation, Supervision. **Shumin Liu:** Writing – review & editing, Funding acquisition, Conceptualization. **Fang Lu:** Writing – review & editing, Validation.

Declaration of competing interest

The authors declare the following financial interests/personal relationships which may be considered as potential competing interests:Shumin Liu reports financial support was provided by Heilongjiang University of Chinese Medicine. Shumin Liu reports a relationship with Heilongjiang University of Chinese Medicine that includes: funding grants. If there are other authors, they declare that they have no known competing financial interests or personal relationships that could have appeared to influence the work reported in this paper.

Acknowledgements

This work was supported by Heilongjiang Postdoctoral Program (No. ZHY2022-114),General program of Heilongjiang Province (No. LBHZ22251).

Abbreviations

AS Atherosclerosis

OX-LDL	oxidized low-density lipoprotein
HFD	high fat diet; BA:bile acids
HQCFT	Huang Qi Chi Feng decoction
ALT	alanine aminotransferase
AST	aspartate aminotransferase
ALP	alkaline phosphatase
TC	total cholesterol(TC)
TG	triglycerides(TG)
LDL-C	low-density lipoprotein cholesterol
HDL-C	high-density lipoprotein cholesterol
PCoA	Principal Co-ordinates Analysis
LEfSe	Linear Discriminant Analysis Effect Size
UDCA	ursodeoxycholic acid
HCA	hyocholic acid
LCA	lithocholic acid
DCA	deoxycholic acid(DCA)
HDCA	hyodeoxycholic acid
TDCA	taurodeoxycholic acid
TLCA	taurolithocholic acid
GDCA	glycodeoxycholic acid
FXR	Farnesoid X receptor
LPS	lipopolysaccharide
SCFAs	short-chain fatty acids
CA	Cholic Acid
CDCA	Chenodeoxycholic Acid
BSH	bile salt hydrolase
FGF15	Fibroblast Growth Factor 15
LXRα	Liver X Receptor α
ABCA1	ATP-binding cassette transporter A1
ABCG1	ATP-binding cassette transporter G1.

Appendix A. Supplementary data

Supplementary data related to this article can be found at https://doi.org/10.1016/j.heliyon.2023.e21935.

References

[1] O. Soehnlein, P. Libby, Targeting inflammation in atherosclerosis - from experimental insights to the clinic, Nat. Rev. Drug Discov. 20 (2021) 589–610, https://doi.org/10.1038/s41573-021-00198-1.

[2] B. Legein, L. Temmerman, E.A.L. Biessen, E. Lutgens, Inflammation and immune system interactions in atherosclerosis, Cell. Mol. Life Sci. 70 (2013) 3847–3869, https://doi.org/10.1007/s00018-013-1289-1.

[3] M.M. Kavurma, K.J. Rayner, D. Karunakaran, The walking dead: macrophage inflammation and death in atherosclerosis, Curr. Opin. Lipidol. 28 (2017) 91–98, https://doi.org/10.1097/MOL.0000000000000394.

[4] S. Ma, B. Yang, M. Zhao, P. Li, J. Fan, M. Chang, Z. Pan, Z. Zhang, S. Xue, Y. Zhang, Effects of modified Huangqi Chifeng decoction on the IL-17 signaling pathway in an IgA nephropathy rat model, J. Ethnopharmacol. 307 (2023), 116220, https://doi.org/10.1016/j.jep.2023.116220.

[5] M. Zhao, B. Yang, L. Li, Y. Si, M. Chang, S. Ma, R. Li, Y. Wang, Y. Zhang, Efficacy of Modified Huangqi Chifeng decoction in alleviating renal fibrosis in rats with IgA nephropathy by inhibiting the TGF-β1/Smad 3 signaling pathway through exosome regulation, J. Ethnopharmacol. 285 (2022), 114795, https://doi.org/10.1016/j.jep.2021.114795.

[6] W.H.W. Tang, Z. Wang, B.S. Levison, R.A. Koeth, E.B. Britt, X. Fu, Y. Wu, S.L. Hazen, Intestinal microbial metabolism of phosphatidylcholine and cardiovascular risk, N. Engl. J. Med. 368 (2013) 1575–1584, https://doi.org/10.1056/NEJMoa1109400.

[7] Q.Y. Wang, N. Zhang, S.Y. Liu, X.H. Jiang, S.M. Liu, Saposhnikoviae Radix enhanced the angiogenic and anti-inflammatory effects of Huangqi Chifeng tang in a rat model of cerebral infarction, Evid. base Compl. Alternative Med. (2021) 1–12, https://doi.org/10.1155/2021/4232708, 2021.

[8] S.Y. Liu, Q.Y. Wang, S.M. Liu, The therapeutic effect of Huangqi Chifeng Decoction on the expression of ZO-1, Claudin-5, P-gp and MRP1 protein in cerebral infarction rat model, Chin. J. Exp. Tradit. Med. Formulae 28 (2022) 26–33, https://doi.org/10.13422/j.cnki.syfjx.20220643.

[9] A.C. Gomes, C. Hoffmann, J.F. Mota, The human gut microbiota: metabolism and perspective in obesity, Gut Microb. 9 (2018) 308–325, https://doi.org/10.1080/19490976.2018.1465157.

[10] J. Fu, M.J. Bonder, M.C. Cenit, E.F. Tigchelaar, A. Maatman, J.A.M. Dekens, E. Brandsma, J. Marczynska, F. Imhann, R.K. Weersma, L. Franke, T.W. Poon, R. J. Xavier, D. Gevers, M.H. Hofker, C. Wijmenga, A. Zhernakova, The gut microbiome contributes to a substantial proportion of the variation in blood lipids, Circ. Res. 117 (2015) 817–824, https://doi.org/10.1161/CIRCRESAHA.115.306807.

[11] X. Jia, W. Xu, L. Zhang, X. Li, R. Wang, S. Wu, Impact of gut microbiota and microbiota-related metabolites on hyperlipidemia, Front. Cell. Infect. Microbiol. 11 (2021), 634780, https://doi.org/10.3389/fcimb.2021.634780.

[12] S. Fiorucci, M. Baldoni, P. Ricci, A. Zampella, E. Distrutti, M. Biagioli, Bile acid-activated receptors and the regulation of macrophages function in metabolic disorders, Curr. Opin. Pharmacol. 53 (2020) 45–54, https://doi.org/10.1016/j.coph.2020.04.008.

[13] C. Kf, D. Pe, A. Ht, K. Pa, Polyphenol effects on cholesterol metabolism via bile acid biosynthesis, CYP7A1: a review, Nutrients 11 (2019), https://doi.org/10.3390/nu11112588.

[14] Y. Kusumoto, J. Irie, K. Iwabu, H. Tagawa, A. Itoh, M. Kato, N. Kobayashi, K. Tanaka, R. Kikuchi, M. Fujita, Y. Nakajima, K. Morimoto, T. Sugizaki, S. Yamada, T. Kawai, M. Watanabe, Y. Oike, H. Itoh, Bile acid binding resin prevents fat accumulation through intestinal microbiota in high-fat diet-induced obesity in mice, Metabolism 71 (2017) 1–6, https://doi.org/10.1016/j.metabol.2017.02.011.

[15] Y. Wang, L. Zheng, Z. Zhou, D. Yao, Y. Huang, B. Liu, Y. Duan, Y. Li, Review article: insights into the bile acid-gut microbiota axis in intestinal failure-associated liver disease-redefining the treatment approach, Aliment. Pharmacol. Ther. 55 (2022) 49–63, https://doi.org/10.1111/apt.16676.

[16] Q.Y. Wang, S.M. Liu, Study on extraction technology of Huangqi Chifeng decoction, West China Pharmaceutical Journal 37 (2022) 311–314, https://doi.org/10.13375/j.cnki.wcjps.2022.03.017.

[17] D. Mauricio, E. Castelblanco, N. Alonso, Cholesterol and inflammation in atherosclerosis: an immune-metabolic hypothesis, Nutrients 12 (2020) 2444, https://doi.org/10.3390/nu12082444.

[18] A.L. Jonsson, F. Bäckhed, Role of gut microbiota in atherosclerosis, Nat. Rev. Cardiol. 14 (2017) 79–87, https://doi.org/10.1038/nrcardio.2016.183.

[19] M. Vourakis, G. Mayer, G. Rousseau, The role of gut microbiota on cholesterol metabolism in atherosclerosis, Int. J. Mol. Sci. 22 (2021) 8074, https://doi.org/10.3390/ijms22158074.

[20] W.H.W. Tang, T. Kitai, S.L. Hazen, Gut Microbiota in Cardiovascular Health and Disease, Circ Res. 120 (2017) 1183–1196, https://doi.org/10.1161/CIRCRESAHA.117.309715.

[21] A. Al Samarraie, M. Pichette, G. Rousseau, Role of the gut microbiome in the development of atherosclerotic cardiovascular disease, Int. J. Mol. Sci. 24 (2023) 5420, https://doi.org/10.3390/ijms24065420.

[22] Y. Wang, W.-X. Ding, T. Li, Cholesterol and bile acid-mediated regulation of autophagy in fatty liver diseases and atherosclerosis, Biochim. Biophys. Acta Mol. Cell Biol. Lipids 1863 (2018) 726–733, https://doi.org/10.1016/j.bbalip.2018.04.005.

[23] J.Y.L. Chiang, J.M. Ferrell, Y. Wu, S. Boehme, Bile acid and cholesterol metabolism in atherosclerotic cardiovascular disease and therapy, Cardiol. 5 (2020) 159–170.

[24] S. Fiorucci, E. Distrutti, Bile acid-activated receptors, intestinal microbiota, and the treatment of metabolic disorders, Trends Mol. Med. 21 (2015) 702–714, https://doi.org/10.1016/j.molmed.2015.09.001.

[25] M. Schoeler, R. Caesar, Dietary lipids, gut microbiota and lipid metabolism, Rev. Endocr. Metab. Disord. 20 (2019) 461–472, https://doi.org/10.1007/s11154-019-09512-0.

[26] J. Yin, Y. Li, H. Han, S. Chen, J. Gao, G. Liu, X. Wu, J. Deng, Q. Yu, X. Huang, R. Fang, T. Li, R.J. Reiter, D. Zhang, C. Zhu, G. Zhu, W. Ren, Y. Yin, Melatonin reprogramming of gut microbiota improves lipid dysmetabolism in high-fat diet-fed mice, J. Pineal Res. 65 (2018), e12524, https://doi.org/10.1111/jpi.12524.

[27] W. Zhu, J.C. Gregory, E. Org, J.A. Buffa, N. Gupta, Z. Wang, L. Li, X. Fu, Y. Wu, M. Mehrabian, R.B. Sartor, T.M. McIntyre, R.L. Silverstein, W.H.W. Tang, J. A. DiDonato, J.M. Brown, A.J. Lusis, S.L. Hazen, Gut microbial metabolite TMAO enhances platelet hyperreactivity and thrombosis risk, Cell 165 (2016) 111–124, https://doi.org/10.1016/j.cell.2016.02.011.

[28] J.Y.L. Chiang, Bile acid metabolism and signaling, Compr. Physiol. 3 (2013) 1191–1212, https://doi.org/10.1002/cphy.c120023.

[29] T. Li, J.Y.L. Chiang, Bile acid signaling in metabolic disease and drug therapy, Pharmacol. Rev. 66 (2014) 948–983, https://doi.org/10.1124/pr.113.008201.

[30] L. Sun, Y. Pang, X. Wang, Q. Wu, H. Liu, B. Liu, G. Liu, M. Ye, W. Kong, C. Jiang, Ablation of gut microbiota alleviates obesity-induced hepatic steatosis and glucose intolerance by modulating bile acid metabolism in hamsters, Acta Pharm. Sin. B 9 (2019) 702–710, https://doi.org/10.1016/j.apsb.2019.02.004.

[31] P.G. Wolf, S. Devendran, H.L. Doden, L.K. Ly, T. Moore, H. Takei, H. Nittono, T. Murai, T. Kurosawa, G.E. Chlipala, S.J. Green, G. Kakiyama, P. Kashyap, V. J. McCracken, H.R. Gaskins, P.M. Gillevet, J.M. Ridlon, Berberine alters gut microbial function through modulation of bile acids, BMC Microbiol. 21 (2021) 24, https://doi.org/10.1186/s12866-020-02020-1.

[32] A.A. Goldberg, A. Beach, G.F. Davies, T.A.A. Harkness, A. Leblanc, V.I. Titorenko, Lithocholic bile acid selectively kills neuroblastoma cells, while sparing normal neuronal cells, Oncotarget 2 (2011) 761–782, https://doi.org/10.18632/oncotarget.338.

[33] L.K. Stenman, R. Holma, R. Korpela, High-fat-induced intestinal permeability dysfunction associated with altered fecal bile acids, World J. Gastroenterol. 18 (2012) 923–929, https://doi.org/10.3748/wjg.v18.i9.923.

[34] B.P. Willing, J. Dicksved, J. Halfvarson, A.F. Andersson, M. Lucio, Z. Zheng, G. Järnerot, C. Tysk, J.K. Jansson, L. Engstrand, A pyrosequencing study in twins shows that gastrointestinal microbial profiles vary with inflammatory bowel disease phenotypes, Gastroenterology 139 (2010) 1844–1854.e1, https://doi.org/10.1053/j.gastro.2010.08.049.

[35] J. T, K. Jy, S. P, W. Bp, Defining the role of Parasutterella, a previously uncharacterized member of the core gut microbiota, ISME J. 13 (2019), https://doi.org/10.1038/s41396-019-0364-5.

[36] Y.-J. Chen, H. Wu, S.-D. Wu, N. Lu, Y.-T. Wang, H.-N. Liu, L. Dong, T.-T. Liu, X.-Z. Shen, Parasutterella, in association with irritable bowel syndrome and intestinal chronic inflammation, J. Gastroenterol. Hepatol. 33 (2018) 1844–1852, https://doi.org/10.1111/jgh.14281.

[37] S. Adhikary, W. Nicklas, M. Bisgaard, R. Boot, P. Kuhnert, T. Waberschek, B. Aalbæk, B. Korczak, H. Christensen, Rodentibacter gen. nov. including Rodentibacter pneumotropicus comb. nov., Rodentibacter heylii sp. nov., Rodentibacter myodis sp. nov., Rodentibacter ratti sp. nov., Rodentibacter heidelbergensis sp. nov., Rodentibacter trehalosifermentans sp. nov., Rodentibacter rarus sp. nov., Rodentibacter mrazii and two genomospecies, Int. J. Syst. Evol. Microbiol. 67 (2017) 1793–1806, https://doi.org/10.1099/ijsem.0.001866.

[38] A. Jin, Y. Zhao, Y. Yuan, S. Ma, J. Chen, X. Yang, S. Lu, Q. Sun, Single treatment of vitamin D3 ameliorates LPS-induced acute lung injury through changing lung rodentibacter abundance, Mol. Nutr. Food Res. 66 (2022), e2100952, https://doi.org/10.1002/mnfr.202100952.

[39] K. Wang, M. Liao, N. Zhou, L. Bao, K. Ma, Z. Zheng, Y. Wang, C. Liu, W. Wang, J. Wang, S.-J. Liu, H. Liu, Parabacteroides distasonis alleviates obesity and metabolic dysfunctions via production of succinate and secondary bile acids, Cell Rep. 26 (2019) 222–235.e5, https://doi.org/10.1016/j.celrep.2018.12.028.

[40] C. Serena, V. Ceperuelo-Mallafré, N. Keiran, M.I. Queipo-Ortuño, R. Bernal, R. Gomez-Huelgas, M. Urpi-Sarda, M. Sabater, V. Pérez-Brocal, C. Andrés-Lacueva, A. Moya, F.J. Tinahones, J.M. Fernández-Real, J. Vendrell, S. Fernández-Veledo, Elevated circulating levels of succinate in human obesity are linked to specific gut microbiota, ISME J. 12 (2018) 1642–1657, https://doi.org/10.1038/s41396-018-0068-2.

[41] Y. Wang, C. Wang, J. Huang, M. Xie, X. Li, L. Fu, *Butyricicoccus* plays a key role in mediating the antagonism between probiotic and antibiotic on food allergy, Food Agric. Immunol. 30 (2019) 446–461, https://doi.org/10.1080/09540105.2019.1594704.

[42] A. Loy, C. Pfann, M. Steinberger, B. Hanson, S. Herp, S. Brugiroux, J.C. Gomes Neto, M.V. Boekschoten, C. Schwab, T. Urich, A.E. Ramer-Tait, T. Rattei, B. Stecher, D. Berry, Lifestyle and horizontal gene transfer-mediated evolution of Mucispirillum schaedleri, a core member of the murine gut microbiota, mSystems 2 (2017) 001711–e216, https://doi.org/10.1128/mSystems.00171-16.

[43] D. Rizzolo, B. Kong, R.E. Taylor, A. Brinker, M. Goedken, B. Buckley, G.L. Guo, Bile acid homeostasis in female mice deficient in Cyp7a1 and Cyp27a1, Acta Pharm. Sin. B 11 (2021) 3847–3856, https://doi.org/10.1016/j.apsb.2021.05.023.

[44] K.E. Bove, J.E. Heubi, W.F. Balistreri, K.D.R. Setchell, Bile acid synthetic defects and liver disease: a comprehensive review, Pediatr. Dev. Pathol. 7 (2004) 315–334, https://doi.org/10.1007/s10024-002-1201-8.

[45] A. Wahlström, S.I. Sayin, H.-U. Marschall, F. Bäckhed, Intestinal crosstalk between bile acids and microbiota and its impact on host metabolism, Cell Metabol. 24 (2016) 41–50, https://doi.org/10.1016/j.cmet.2016.05.005.

[46] S.I. Sayin, A. Wahlström, J. Felin, S. Jäntti, H.-U. Marschall, K. Bamberg, B. Angelin, T. Hyötyläinen, M. Orešič, F. Bäckhed, Gut microbiota regulates bile acid metabolism by reducing the levels of tauro-beta-muricholic acid, a naturally occurring FXR antagonist, Cell Metabol. 17 (2013) 225–235, https://doi.org/10.1016/j.cmet.2013.01.003.

[47] K.M. Schneider, L.S. Candels, J.R. Hov, M. Myllys, R. Hassan, C.V. Schneider, A. Wahlström, A. Mohs, S. Zühlke, L. Liao, C. Elfers, K. Kilic, M. Henricsson, A. Molinaro, M. Hatting, A. Zaza, D. Drasdo, M. Frissen, A.S. Devlin, E.J.C. Gálvez, T. Strowig, T.H. Karlsen, J.G. Hengstler, H.-U. Marschall, A. Ghallab, C. Trautwein, Gut microbiota depletion exacerbates cholestatic liver injury via loss of FXR signalling, Nat. Metab. 3 (2021) 1228–1241, https://doi.org/10.1038/s42255-021-00452-1.

[48] T. Wang, Y. Zhao, Z. You, X. Li, M. Xiong, H. Li, N. Yan, Endoplasmic reticulum stress affects cholesterol homeostasis by inhibiting LXRα expression in hepatocytes and macrophages, Nutrients 12 (2020) 3088, https://doi.org/10.3390/nu12103088.

[49] L. Zhao, W. Lei, C. Deng, Z. Wu, M. Sun, Z. Jin, Y. Song, Z. Yang, S. Jiang, M. Shen, Y. Yang, The roles of liver X receptor α in inflammation and inflammation-associated diseases, J. Cell. Physiol. 236 (2021) 4807–4828, https://doi.org/10.1002/jcp.30204.

[50] J. Lyu, H. Imachi, K. Fukunaga, S. Sato, T. Kobayashi, T. Dong, T. Saheki, M. Matsumoto, H. Iwama, H. Zhang, K. Murao, Role of ATP-binding cassette transporter A1 in suppressing lipid accumulation by glucagon-like peptide-1 agonist in hepatocytes, Mol. Metabol. 34 (2020) 16–26, https://doi.org/10.1016/j.molmet.2019.12.015.

[51] M.M. Babashamsi, S.Z. Koukhaloo, S. Halalkhor, A. Salimi, M. Babashamsi, ABCA1 and metabolic syndrome; a review of the ABCA1 role in HDL-VLDL production, insulin-glucose homeostasis, inflammation and obesity, Diabetes Metabol. Syndr. 13 (2019) 1529–1534, https://doi.org/10.1016/j.dsx.2019.03.004.

[52] A.D. Dergunov, E.V. Savushkin, L.V. Dergunova, D.Y. Litvinov, Significance of cholesterol-binding motifs in ABCA1, ABCG1, and SR-B1 structure, J. Membr. Biol. 252 (2019) 41–60, https://doi.org/10.1007/s00232-018-0056-5.